

Supporting Information for:

Anthracyclines React with Apurinic/Apyrimidinic Sites in DNA

Medjda Bellamri,^{1,2} John T. Terrell,³ Kyle Brandt,^{1,2} Francesca Gruppi,³ Robert J. Turesky,
^{1,2} and Carmelo J Rizzo*^{3,4,5}*

¹Masonic Cancer Center and ²Department of Medicinal Chemistry, University of Minnesota, Minneapolis, MN 55455, United States and ³Departments of Chemistry and ⁴Biochemistry, and ⁵Vanderbilt-Ingram Cancer Center, Vanderbilt University, Nashville, TN 37235-1822, United States

Email: rturesky@umn.edu or c.rizzo@vanderbilt.edu

Supporting Information Table of Contents

Methods and Procedures	S4
<i>Chemicals and Reagents</i>	S4
<i>Reaction of anthracyclines with an AP-containing double-stranded 12mer oligonucleotide in the presence of NaB(CN)H₃</i>	S5
<i>Enzymatic digestion of the reduced anthracycline-conjugated 12mer oligonucleotides</i>	S6
<i>Synthesis of reduced anthracycline-dR conjugate standards</i>	S7
<i>Monitoring AP sites levels in CT-DNA during NaB(CN)H₃ reduction of the MTX-dR-Schiff base in CT DNA</i>	S11
<i>Enzymatic digestion of DNA containing reduced MTX-dR</i>	S11
<i>SPE enrichment of reduced MTX-dR</i>	S11
<i>LC/MS³ measurement of reduced MTX-dR</i>	S12
<i>LC/MS² method for detection of PMOA-dR</i>	S12
<i>MTX uptake in nuclear DNA of MDA-MB-231</i>	S13
<i>Calibration curves and limits of MTX-dR and MTX detection in CT DNA</i>	S14
<i>Statistics</i>	S16
<i>References</i>	S16
Scheme S1. Previously proposed mechanisms of covalent modification of DNA by anthracyclines	S17

Figure S1.	Reaction of anthracyclines with an AP-containing 12mer DNA duplex in the presence of NaB(CN)H ₃ after 24 h	S18
Figure S2.	Mass spectrum of 5'-GTT GCN CGT ATG-3' where N is the reduced DOX-dR conjugate.....	S19
Figure S3.	CID mass spectrum of the <i>m/z</i> 1360.9 (–3) ion of 5'-GTT GCN CGT ATG-3' where N is the reduced DOX-dR conjugate.....	S20
Figure S4.	CID mass spectrum of the <i>m/z</i> 1020.5 (–4) ion of 5'-GTT GCN CGT ATG-3' where N is the reduced DOX-dR conjugate.....	S21
Figure S5.	CID mass spectrum of the <i>m/z</i> 816.2 (–5) ion of 5'-GTT GCN CGT ATG-3' where N is the reduced DOX-dR conjugate.....	S22
Table S1.	CID fragment ions from 5'-GTT GCN CGT ATG-3' where N is the reduced DOX-dR conjugate.....	S23
Figure S6.	Mass spectrum of 5'-GTT GCN CGT ATG-3' where N is the reduced EPI-dR conjugate.....	S24
Figure S7.	CID mass spectrum of the <i>m/z</i> 1360.9 (–3) ion of 5'-GTT GCN CGT ATG-3' where N is the reduced EPI-dR conjugate.....	S25
Figure S8.	CID mass spectrum of the <i>m/z</i> 1020.5 (–4) ion of 5'-GTT GCN CGT ATG-3' where N is the reduced EPI-dR conjugate.....	S26
Figure S9.	CID mass spectrum of the <i>m/z</i> 816.2 (–5) ion of 5'-GTT GCN CGT ATG-3' where N is the reduced EPI-dR conjugate.....	S27
Table S2.	CID fragment ions from 5'-GTT GCN CGT ATG-3' where N is the reduced EPI-dR conjugate.....	S28
Figure S10.	Mass spectrum of 5'-GTT GCN CGT ATG-3' where N is the reduced MTX-dR conjugate.....	S29
Figure S11.	CID mass spectrum of the <i>m/z</i> 1327.9 (–3) ion of 5'-GTT GCN CGT ATG-3' where N is the reduced MTX-dR conjugate.....	S30
Figure S12.	CID mass spectrum of the <i>m/z</i> 796.4 (–5) ion of 5'-GTT GCN CGT ATG-3' where N is the reduced MTX-dR conjugate.....	S31
Figure S13.	CID mass spectrum of the <i>m/z</i> 995.6 (–4) ion of 5'-GTT GCN CGT ATG-3' where N is the reduced MTX-dR conjugate.....	S32
Table S3.	CID fragment ions from 5'-GTT GCN CGT ATG-3' where N is the reduced EPI-dR conjugate.....	S33
Figure S14.	Mass spectrum of 5'-GTT GCN CGT ATG-3' where N is the reduced PIX-dR conjugate.....	S34
Figure S15.	CID mass spectrum of the <i>m/z</i> 1288.1 (–3) ion of 5'-GTT GCN CGT ATG-3' where N is the reduced PIX-dR conjugate.....	S35
Figure S16.	CID mass spectrum of the <i>m/z</i> 966.0 (–4) ion of 5'-GTT GCN CGT ATG-3' where N is the reduced MTX-dR conjugate.....	S36
Figure S17.	CID mass spectrum of the <i>m/z</i> 722.6 (–5) ion of 5'-GTT GCN CGT ATG-3' where N is the reduced PIX-dR conjugate.....	S37
Table S4.	CID fragment ions from 5'-GTT GCN CGT ATG-3' where N is the reduced PIX-dR conjugate.....	S38

Figure S18.	Extracted ion chromatograms of the enzymatic digestion of the reduced DOX-dR containing 12-mer oligonucleotide (5'-GTT GCN CGT ATG-3')	S39
Figure S19.	Extracted ion chromatograms of the enzymatic digestion of the reduced EPI-dR containing 12-mer oligonucleotide (5'-GTT GCN CGT ATG-3')	S40
Figure S20.	Extracted ion chromatograms of the enzymatic digestion of the reduced PIX-dR containing 12-mer oligonucleotide (5'-GTT GCN CGT ATG-3')	S41
Figure S21.	Extracted ion chromatograms of the enzymatic digestion of the reduced MTX-dR containing 12-mer oligonucleotide.....	S42
Figure S22.	600 MHz ¹ H NMR spectra of reduced MTX-dR	S43
Figure S23.	Full scan MS, and CID MS ² and MS ³ spectra of reduced MTX-[¹³ C ₅]dR.....	S44
Figure S24.	600 MHz ¹ H NMR spectra of reduced DOX-dR.....	S45
Figure S25.	600 MHz ¹ H NMR spectra of the reduced EPI-dR	S46
Figure S26.	600 MHz ¹ H NMR spectra of the reduced PIX-dR	S47
Figure S27.	Full scan (top) and CID (bottom) mass spectra of reduced DOX-dR	S48
Figure S28.	Full scan (top) and CID (bottom) mass spectra of the reduced EPI-dR	S49
Figure S29.	Full scan (top) and CID (bottom) mass spectra (<i>m/z</i> 444.3 ion) of the reduced PIX-dR conjugate.....	S50
Figure S30.	The calibration curve for reduced MTX-dR was constructed within a CT DNA digest matrix.....	S51
Figure S31.	A calibration curve for MTX was constructed within a CT DNA digest matrix	S52
Figure S32.	Kinetics of MTX-dR Schiff base formation in CT DNA reduced with NaB(CN)H ₃	S53
Figure S33.	Time course for AP Site formation in MDA-MB-231 breast cancer cell after co-treatment with NNM and MTX	S54
Figure S34.	Reduced MTX-dR levels formed over time in NNM and MTX treated MDA-MB-231 cells isolated nuclei	S55
Figure S35.	Time course for formation of reduced MTX-dR levels and AP sites in the isolated nuclei of MDA-MB-231 cells co-treated with NNM and MTX over 18 h.....	S56
Figure S36.	MTX uptake in nuclei isolated from MDA-MB-231 cells treated with various concentrations of MTX for 24 h	S57
Figure S37.	Full scan MS, MS ² and MS ³ spectra for MTX isolated from treated MDA-MB-231 cells	S58
Figure S38.	LC/MS ³ chromatograms of MTX uptake in cells and CID MS ³ mass spectra of MTX and [² H ₈]-MTX	S59
Figure S39.	MS fragment ion nomenclature for oligonucleotides.....	S60

Methods and Procedures.

Chemical and reagents. Mitoxantrone (MTX), [$^2\text{H}_8$]-Mitoxantrone ([$^2\text{H}_8$]-MTX) and Bis(2-chloroethyl)amine hydrochloride (nornitrogen mustard, NNM) were purchased from Toronto Research Chemicals, Ontario, Canada. $^{13}\text{C}_5$ -deoxyribose (98.9% isotopic purity) was purchased for Santa Cruz Biotechnology (Dallas, TX). O-(pyridin-3-ylmethyl)hydroxylamine (PMOA), butyraldehyde, 4-(2-hydroxyethyl)-1-piperazineethanesulfonic acid (HEPES), calf thymus (CT) DNA RNase A (bovine pancreas), RNase T1 (*Aspergillus oryzae*), proteinase K (*Tritirachium album*), sodium dodecyl sulfate (SDS), DNase I (type IV, bovine pancreas), alkaline phosphatase (*Escherichia coli*), and nuclease P1 (*Penicillium citrinum*) were purchased from Sigma Aldrich (St. Louis, MO, USA). Phosphodiesterase I (*Crotalus adamanteus* venom) and adenosine deaminase were purchased from Worthington Biochemical Corp. (Newark, NJ). LC/MS grade solvents were purchased from Fisher Chemical Co. (Pittsburgh, PA). Puregene protein precipitation solution was purchased from Qiagen (Germantown, MD). Strata-X 33 μm Polymeric Reversed Phase 30 mg SPE cartridges were obtained from Phenomenex (Torrance, CA, USA). Sola HRP Polymeric Reversed Phase 10 mg SPE cartridges were purchased from Thermo Fisher Scientific (San Jose, CA, USA). Optima LC-MS grade water and acetonitrile were purchased from Thermo Fisher Scientific (Waltham, MA). All other chemicals were purchased from Sigma-Aldrich (St. Louis, MO), if not stated otherwise.

Reaction of anthracyclines with an AP-containing double-stranded 12mer oligonucleotide in the presence of $\text{NaB}(\text{CN})\text{H}_3$ and MS analyses. A typical procedure is given for the reaction of MTX with the AP-containing 12mer duplex. The uracil-containing 12mer oligonucleotide (10 nmol, 5'-GTT GCU CGT ATG-3') was combined with its complementary strand (10 nmol, 5'-CAT ACG CGC AAC-3') in HEPES buffer (total volume

was 500 μL). The solution was heated to 90 $^{\circ}\text{C}$ for 5 min, and the strands annealed by allowing the solution to cool slowly to ambient temperature. UDG (0.25 units/ μL) was added and the mixture heated to 37 $^{\circ}\text{C}$ for 1 h. MTX (11 μL of a 0.002 M stock solution, 0.04 mM final concentration) was added simultaneously with $\text{NaB}(\text{CN})\text{H}_3$ (28 μL of a freshly prepared 1 M solution in water, 50 mM final concentration). The reaction was allowed to incubate at 37 $^{\circ}\text{C}$ for 3 h, then purified by reversed-phase HPLC (Luna Clarity[®] Oligo-RP, 4.6 x 250 mm ID, 10 μm particle size, 100 \AA pore size, Phenomenex, Torrance, CA) at a flow rate of 1.5 mL/min using the following solvent conditions. Solvent **A**: 0.1 M ammonium formate; Solvent **B**: acetonitrile. Gradient from 1% to 10% **B** over 15 min, followed by 10% to 20% **B** over 5 min, then increased to 80% **B** over 2 min, held isocratic at 80% **B** for 3 min, then decreased to 0% **B** over 2 min then held isocratic at 0% **B** for 3 min.

The modified oligonucleotides were analyzed by LC/MS on a Waters Acquity UPLC system (Waters, Milford, MA) connected to a Finnigan LTQ ion trap mass spectrometer (Thermo Electron, San Jose, CA) equipped with an *Ion Max* API source and a standard electrospray probe. Separation was performed by C_{18} -reversed-phase HPLC (Luna, 2 x 150 mm, 3 μm particle size, 100 \AA pore size, Phenomenex, Torrance, CA) at a flow rate of 0.125 mL/min using the following solvent conditions: **A**: 1% acetonitrile in water containing 0.01 M ammonium acetate, **B**: 90% acetonitrile in water containing 0.01 M ammonium acetate: initial 0% **B**, isocratic for 1 min; linear gradient to 5% **B** over 3 min; linear gradient to 20% **B** over 2 min; linear gradient to 40% **B** over 1 min; linear gradient to 50% **B** over 2 min followed by an increase to 100% **B** over 1 min and held isocratic for 1 min, then decreased to 0% **B** over 1 min and held isocratic for 6 min for re-equilibration, then returned to original conditions. Identification was conducted in negative ion mode using the triply and quadruply charged ion species. The MS source parameters were: N_2 sheath gas pressure was 36 psi; N_2 auxiliary

gas pressure was 37 psi; spray voltage was 4.0 kV; tube lens voltage was -53.12 V; capillary voltage was -5.0 V; capillary temperature 300° C; the normalized capillary-induced dissociation was 35% for MS²; activation Q was 0.25; 1 microscan, AGC max inject time was 100 ms; the isolation width was m/z 3.0 for MS². The Mongo Oligo Mass Calculator (v. 2.06, <http://rna.rega.kuleuven.be/masspec/mongo.htm>) was used to calculate the theoretical electrospray mass series (**Figures S2, S6, S10, and S14**) and the a-b and w fragment ions¹ (**Figures S3-S5, S7-S9, S11-S13, and S15-17**). The theoretical m/z values were compared to the experimental spectra (**Tables S1-S4**). See the Figure S40 for the ion nomenclature.¹

Enzymatic digestion and MS analysis of the reduced anthracycline-conjugated 12mer oligonucleotides.

The modified oligonucleotides were enzymatically digested as previously described² and the hydrolysate was analyzed by LC/ESI/MS³ employing a Waters Acquity HPLC system (Waters, Milford, MA). The digested products were analyzed on an LTQ linear ion trap mass spectrometer employing the *Ion Max* API electrospray source with separation performed by C₁₈-reversed-phase HPLC (Luna, 2 x 150 mm, 3 μm particle size, 100 Å pore size, Phenomenex, Torrance, CA). The flow rate was 0.125 mL/min using the following solvent conditions: **A:** 0.05% FA, **B:** 95% acetonitrile containing 0.05% FA: initial 2% B, isocratic for 2.5 min; linear gradient to 15% B over 6 min; linear gradient to 40% B over 4 min followed by an increase to 100% B. isocratic for 5 min, then decreased to 0% B, isocratic for 6 min for re-equilibration, then return to original conditions. MS analyses was conducted in positive ion mode using the same parameters as above for the anthracycline-AP conjugated 12-mers noted above with the following modifications: N₂ sheath gas pressure was 44 psi; N₂ auxiliary gas pressure was 21 psi; spray voltage was 5.0 kV; tube lens voltage was 55 V; capillary voltage was 28.5 V; 3 microscans, AGC max inject time was 10 ms. The MS² transitions parameters for unmodified deoxynucleosides ([M+H – 116 Da]⁺) are:

MS² **dC**: m/z 228.1 → 112.1; **dT**: m/z 243.0 → 127.2; **dA**: m/z 252.1 → 136.1; **dG**:
 m/z 268.1 → 152.1

The MS² and MS³ transitions for the reduced anthracycline-dR conjugates:

reduced **DOX-dR** [M+H]⁺ (**Figure S18**): MS² m/z 664.1 → 248.2

reduced **EPI-dR** [M+H]⁺ (**Figure S19**): MS² m/z 664.1 → 248.2

reduced **PIX-dR** [M+H]⁺ (**Figure S20**): MS² m/z 444.2 → 427.2, 384.2, 309.2, 292.2,
266.2, 179.2, 162.2, 136.2

Reduced **MTX-dR** [M+H]⁺ (**Figure S21**): MS² m/z 563.3 → 476.3, 206.2; MS³
[M+2H]²⁺: m/z 282.2 → 476.3 → 297.1, 206.2

Synthesis of reduced anthracycline-dR conjugate.

Reduced MTX-dR. Mitoxantrone (50 mg, 0.113 mmol) was mixed with 2-deoxyribose (18 mg, 0.135 mmol) in methanol (4.5 mL, 0.025 M) and stirred for 1h at rt under an argon atmosphere. NaB(CN)H₃ (35 mg, 0.563 mmol) was added, and the reaction stirred at rt for 12 h. The solvent was removed under reduced pressure on a rotary evaporator and the crude product was dissolved in water (5 mL). Initial purification was performed by SPE elution using SOLA HRP cartridges (30 mg/3 mL cartridge size; 250 μ L sample loading in LC/MS-grade water) on a vacuum manifold (Supelco, Visiprep™ 12). Cartridges were preconditioned with 3 mL methanol followed by 3 mL water. After loading the sample, elution was performed by washing with 4 mL water followed by 4 mL of 0.05% formic acid (FA), 4 mL of 8% MeOH in 0.05% FA, and 25% MeOH in 0.05% FA. All fractions were collected, dried, and further purified by C₈-reversed phase HPLC (Luna, 250 x 10 mm ID, 5 μ m pore size, 100 Å particle size) using the following solvent gradient (Solvent **A**: 0.1 M ammonium formate, Solvent **B**: acetonitrile) at a flow rate of 5 mL/min: 18% **B** for 22 min, followed by a linear gradient to 25% **B** over 2 min, then isocratic at 25% **B** for 6 min, followed by return to the original

conditions. MTX-dR was collected as the second major peak eluting between 22-25 min. Identity of the reduced MTX-dR adduct was confirmed by LC/ESI/MS² using the LTQ ion trap MS employing a Waters Acquity UPLC system (Waters, Milford, MA) connected to a Finnigan LTQ mass spectrometer (Thermo Electron) equipped with an *Ion Max* API electrospray source. Samples were run via direct flow monitoring without an attached column. The mobile phase solvent was 50% MeOH/H₂O. The sample (20 μL dissolved in 0.1% FA) was injected and eluted at a 0.25 mL/min flow rate. Identification was conducted in positive ion mode using the singly and doubly charged ion species. The MS source parameters were the same as described above for the enzymatic digestion of the modified oligonucleotides. The MS² transitions for reduced MTX-dR [M+H]⁺ were: *m/z* 563.4 → 476.4, 206.1; MTX-dR [M+2H]²⁺ *m/z* 282.2 → 476.3, 358.3, 273.2, 251.6, 206.2, 89.0 (**Figure 3A**).

¹H-NMR (600 MHz; pyridine-*d*₅) (**Figure S22**): δ 7.40 (s, 2H, **2,3**), 7.31 (s, 2H, **6,7**), 4.44 (dd, 1H, *J* = 3.9, 10.4 Hz, **5'**), 4.38 (td, 1H, *J* = 2.3, 8.1 Hz, **3'**), 4.32 (dd, 1H, *J* = 6.2, 10.3 Hz, **5'**), 4.23 (dd, 1H, *J* = 5.8, 10.1 Hz, **4'**), 4.05 (t, 2H, *J* = 5.8 Hz, **15**), 4.01 (t, 2H, *J* = 5.0 Hz, **11**), 3.63 (m, 2H, **18**), 3.56 (q, 2H, *J* = 5.8 Hz, **14**), 3.18 (m, 1H, **1'**), 3.11 (m, 1H, **1'**), 3.05 (t, 2H, *J* = 6.0 Hz, **13**), 3.01 (m, 2H, **12**), 2.99 (m, 2H, **17**), 2.96 (m, 2H, **16**), 2.47 (m, 1H, **2'**), 2.18 (m, 1H, **2'**).

Reduced PIX-dR. The reduced PIX-dR conjugate was synthesized as a mixture of regioisomers using the procedure described above for the reduced MTX-dR with the following modifications. After evaporation of the reaction, the crude product was dissolved in water and insoluble materials were removed by centrifuge filtration (Ultrafree[®]-MC-HV centrifugal filters; Durapore[®]-PVDF 0.45 μm). Initial purification was by C₈-reversed phase HPLC (Luna, 250 x 10 mm ID, 5 μm pore size, 100 Å particle size) at a flow rate of 5 mL/min

with the following solvent conditions: 14% isocratic **B**. The product was dried by lyophilization and further purified by C₈-reversed phase HPLC (Phenomenex, 250 x 4.6 mm ID, 5 μm pore size, 100 Å particle size) at a flow rate of 1.5 mL/min using the following solvent conditions: 8% **B** isocratic for 40 min. The singly charged reduced PIX-dR was characterized by LC/MS system and *Ion Max* API electrospray source as described above for the reduced MTX-dR. The MS² transitions for reduced PXT-dR were (**Figure S29**): m/z 444.3 → 427.2, 384.2, 309.2, 292.2, 266.2, 179.2, 162.2, 136.2.

¹H-NMR (600 MHz; 0.1% CD₂O₂/D₂O) (**Figure S26**): δ 9.04 (bs, 1H, **1**), 8.90 (bs, 1H, **2**), 7.84 (d, 1H, J = 4.0 Hz, **3**), 6.97 (ds, 2H, **7,8**), 3.77 (m, 1H, **3'**), 3.73 (m, 1H, J = 2.4, 11.0 Hz, **5'**), 3.63 (m, 1H, **3'**), 3.60 (m, 1H, **5'**), 3.56 (bs, 2H), 3.52 (bs, 2H), 3.45 (t, 2H, J = 5.4 Hz), 3.36 (t, 2H, J = 5.8 Hz), 3.33 (m, 2H, **1'**), 2.09 (m, 1H, **2'**), 1.91 (m, 1H, J = 8.45 Hz, **2'**).

Reduced DOX-dR. The reduced DOX-dR conjugate was synthesized as a mixture of diastereomers at the C13-OH using the procedure described above for the reduced PIX-dR with the following modification. The product was purified by C₈-reversed phase HPLC (Luna, 250 x 10 mm ID, 5 μm pore size, 100 Å particle size) at a flow rate of 5 mL/min with the following solvent conditions: 23% **B** isocratic for 15 min. The singly charged reduced DOX-dR was characterized by LC/MS system and *Ion Max* API electrospray source as described above. The MS source parameters were the same as for the reduced MTX-dR with the following modifications: N₂ sheath gas pressure was 36 psi; N₂ auxiliary gas pressure was 37 psi; tube lens voltage was 30 V; capillary voltage was 10 V; 1 microscan, the isolation width was m/z 2.0 for MS². The MS² transition reduced DOX-dR were (**Figure S27**): m/z 664.1 → 248.2.

¹H-NMR (600 MHz; MeOH-*d*₄) mixture of diastereomers (**Figure S24**): δ 8.00 (d, 1H, J = 7.6 Hz, **1**), 7.86 (t, 1H, J = 8.2 Hz, **2**), 7.59 (d, 1H, J = 8.5 Hz, **3**), 5.49 (bs, 0.5H, **1'**), 5.48

(bs, 0.5H, **1'**), 5.15 (bs, 0.5H, **7**), 5.13 (bs, 0.5H, **7**), 4.26 (q, 1H, J = 6.6 Hz, **5'**), 4.04 (s, 3H, **4-OMe**), 3.96 (dd, 1H, J = 3.6, 11.2 Hz, **14**), 3.75 (m, 1H, **4'**), 3.74 (m, 1H, **14**), 3.64 (dd, 1H, J = 4.2, 11.2 Hz, **5''**), 3.61 (m, 1H, **3''**), 3.57 (dd, 1H, J = 3.5, 7.3 Hz, **13**), 3.53 (dd, 1H, J = 6.1, 11.2 Hz, **5''**), 3.44 (m, 1H, J = 4.4, 6.3 Hz, **4''**), 3.34 (m, 1H, **3'**), 3.10 (d, 0.5H, J = 20.6 Hz, **10**), 3.07 (d, 0.5H, J = 18.7 Hz, **10**), 3.03 (m, 2H, **1''**), 2.88 (d, 0.5H, J = 18.7 Hz, **10**), 2.84 (d, 0.5H, J = 20.4 Hz, **10**), 2.49 (d, 0.5H, J = 14.7 Hz, **8**), 2.29 (d, 0.5H, J = 14.0 Hz, **8**), 2.17 (d, 0.5H, J = 14.0 Hz, **8**), 2.01 (dd, 0.5H, J = 4.6, 14.7 Hz, **8**), 1.93 (m, 2H, **2'**), 1.91 (m, 1H, **2''**), 1.75 (m, 1H, J = 7.4 Hz, **2''**), 1.31 (d, 3H, J = 6.4 Hz, **6'**).

Reduced EPI-dR. The reduced EPI-dR conjugate was synthesized as a mixture of diastereomers at the C13-OH using the procedure described above for the reduced DOX-dR. The singly charged reduced EPI-dR was characterized by LC/MS system and *Ion Max* API electrospray source as described above for the reduced DOX-dR. The MS² transition for reduced EPI-dR was (**Figure S28**): m/z 664.1 \rightarrow 248.2.

¹H-NMR (600 MHz; MeOH-*d*₄) mixture of diastereomers (**Figure S25**): δ 7.95 (d, 1H, J = 7.6 Hz, **1**), 7.84 (t, 1H, J = 8.1 Hz, **2**), 7.56 (d, 1H, J = 8.4 Hz, **3**), 5.49 (d, 0.5H, J = 3.2 Hz, **1'**), 5.47 (d, 0.5H, J = 3.2 Hz, **1'**), 5.11 (bs, 0.5H, **7**), 5.09 (bs, 0.5H, **7**), 4.04 (m, 1H, **5'**), 4.03 (s, 3H, **4-OMe**), 3.96 (m, 1H, J = 3.7 Hz, **14**), 3.74 (m, 1H, J = 7.5, 10.9 Hz, **14**), 3.63 (m, 1H, **3''**), 3.60 (m, 1H, **5''**), 3.57 (dd, 1H, J = 3.4, 7.3 Hz, **13**), 3.51 (dd, 1H, J = 6.0, 11.2 Hz, **5''**), 3.45 (m, 1H, J = 4.4, 6.2 Hz, **4''**), 3.27 (m, 1H, **3'**), 3.22 (m, 1H, **4'**), 3.18 (m, 1H, **1''**), 3.08 (d, 0.5H, J = 18.5 Hz, **10**), 3.04 (d, 0.5H, J = 18.5 Hz, **10**), 3.03 (m, 1H, **1''**), 2.85 (d, 0.5H, J = 18.5 Hz, **10**), 2.82 (d, 0.5H, J = 18.5 Hz, **10**), 2.47 (d, 0.5H, J = 14.7 Hz, **8**), 2.33 (m, 1H, **2'**), 2.29 (d, 0.5H, J = 14.8 Hz, **8**), 2.18 (dd, 0.5H, J = 4.8, 14.7 Hz, **8**), 2.02 (dd, 0.5H, J = 4.4, 14.7 Hz, **8**), 1.94 (m, 1H, **2''**), 1.80 (m, 1H, **2'**), 1.79 (m, 1H, **2''**), 1.35 (d, 3H, J = 6.2 Hz, **6'**).

Monitoring AP sites levels in CT-DNA during *NaB(CN)H₃* reduction of the MTX-dR-Schiff base in CT DNA. CT DNA (50 µg) was resuspended in of HEPES buffer (500 µL, 100 mM HEPES, 10 mM NaCl, pH 7.4). PMOA (5 nM final concentration) was added at t 0 min, and the samples were incubated at 37 °C for 30, 60, 90, or 180 min. At each time point, butyraldehyde (30 µmol) was added to quench the reaction, and the samples were incubated at 37 °C at 900 rpm for 10 min. The samples were then placed on ice for 5 min and the DNA was precipitated by adding 0.1 volume NaCl (5 M) and 2 vol of ice chilled isopropanol. The samples were centrifuged at 21,000 × g at 4 °C for 10 min to pellet DNA. DNA was washed twice with 70% ethanol in 5 mM HEPES (pH 8.0) and vacuum centrifuged to dryness. DNA was then digested as described below.

Enzymatic digestion of DNA containing reduced MTX-dR. DNA (10 µg) was spiked with the MTX-[¹³C₅]dR internal standard at a level of 3.7 MTX-dR adducts per 10⁶ nucleotides in Bis-Tris-HCl buffer (100 µL, 5 mM, pH 7.1). DNA was digested with DNase 1 (5 µg) and nuclease P1 (0.5 µg) at 37 °C using a Thermomix at 900 rpm. After 3 h, phosphodiesterase 1 (24 mU) and alkaline phosphatase (40 mU) were added, and the incubation continued for 15 h. Thereafter, the DNA digests were placed on ice for 5 min, and 3 volumes of ice-chilled ethanol was added. The samples were store at -20 °C for 1 h, followed by centrifugation at 21,000 × g 4°C for 10 min. The supernatants were vacuum centrifuged to dryness and resuspended in LC/MS grade H₂O (1 mL) for SPE.

SPE enrichment of reduced MTX-dR. The MTX-dR in the DNA digest was enriched by SPE employing a Sola HRP (10 mg, 1 mL). The SPE cartridge was preconditioned with CH₃OH containing 0.1% FA (2 mL) followed by 0.1% aqueous FA (2 mL). The samples were then loaded on the cartridge and washed with 6% CH₃OH containing 0.1% FA (2 mL). MTX-dR

was eluted from the cartridge with 50% CH₃OH 0.05% FA. Samples were dried by vacuum centrifugation at room temperature, reconstituted in 10% CH₃CN containing 0.1% FA (20 µL), sonicated, and transferred to polypropylene autosampler vials for LC/MS analysis.

LC/MS³ measurement of reduced MTX-dR. The reduced MTX-dR levels were measured by UPLC/ESI/MS³ employing a Velos Pro ion trap mass spectrometer (Thermo Scientific, San Jose, CA) using a Michrom Captive Spray source (Auburn, CA) interfaced to an UltiMate 3000 RSLCnano System (Thermo Fisher Scientific) equipped with a ProntoSIL C18AQ reversed phase column (0.1 × 150 mm, 3 µm particle size, 100 Å pore size, Michrom, Auburn, CA). The mobile phase solvents were (A) 0.01% FA and (B) 95% acetonitrile containing 0.01% FA. The sample (2 µL) was injected onto the analytical column, and the following elution gradient was applied: flow rate, 1.0 µL/min; isocratic at 1% B for 0–3 min; increased to 50% B at 13 min using a linear gradient; then to 99% B at 14 min and held at 99% B for one min. The percentage of the B solvent was reduced 1% B over one min and held at 1% B for 6 min for re-equilibration. The quantitation was conducted in positive ion mode using the doubly charged ion species. The MS source parameters were: spray voltage was 2.0 kV; ion transfer tube temperature was 270 °C; the S-lens RF level was 60%; the normalized collision-induced dissociation (CID) was 30% for both MS² and MS³; activation Q was 0.2; the injection time was 10 ms; the isolation width was m/z 1.0 for both MS² and MS³. Quantification was done in the positive ion mode. The MS³ transitions were: MTX-dR: m/z 282.3 → 476.2 → 206.2; MTX-[¹³C₅]dR: m/z 284.7 → 481.2 → 211.2; [²H₃]MTX-dR: m/z 286.2 > 480.3 > 210.2.

LC/MS² method for detection of PMOA-dR. PMOA-dR was measured on the same LC/MS system and the Advance CaptiveSpray source described above, using the same Magic

C18AQ reversed-phase column for chromatography. The mobile phase solvents were (A) 2 mM NH₄OAc and (B) acetonitrile. The sample (2 μL) was injected onto the analytical column and the following elution gradient was applied: flow rate, 0.7 μL/min; isocratic at 1% B from 0 to 4 min; increased to 66% B at 10 min using a linear gradient; 66 to 99% B from 10 to 12 min; and held at 99% B from 12 to 14 min. The percentage of the B solvent was then reduced from 99 to 1% B over 2 min; and held at 1% B for 6 min for re-equilibration. The MS source parameters were: the spray voltage was 2.0 kV, the ion transfer tube temperature was 275 °C; S-lens RF level was 58%; normalized CID, 30%; activation Q, 0.25; isolation width, *m/z* 2.0. The quantitation was conducted in the positive ion mode. The MS² transitions were: PMOA-dR: *m/z* 241.1 → 92.0, 108.0, 110.0, 125.0. [¹³C₅]PMOA-dR: *m/z* 246.1 → 92.0, 108.0, 110.0, 125.0.³

MTX uptake in nuclear DNA of MDA-MB-231. Cells (1.6×10^6) were seeded in 150 cm² flasks and cultured in complete media for 72 h. Cells were then washed with prewarmed PBS and pretreated with MTX (0.1, 0.3, or 0.6 μM) or 0.1% DMSO (solvent control) for 24 h. After the treatment period, cells were harvested employing trypsin (0.25%) and centrifuged at 600 × g for 7 min. Cell pellets were then washed by cold PBS and stored as dry pellets at -80°C until further use. Cell pellets were resuspended and lysed in lysis buffer (0.5 mL, 250 mM sucrose, 1 mM EDTA, 20 mM HEPES, pH 7.4). Cells were then passed 10 times through a 27-gauge needle and the nuclei were pelleted at 3000 × g at 4 °C for 10 min. The pelleted nuclei were then resuspended in HE buffer (300 μL, 100 mM HEPES, 10 mM EDTA, pH 7.4) and spiked with [²H₈]-MTX (3 nmol). Nuclear pellets were then treated with RNAase A (150 μg) and RNAase T1 (50 U) at 37 °C and 900 rpm. After 90 min, proteinase K (0.4 mg) was added, and the samples were incubated for 24 h at 37 °C using a Thermomixer at 900 rpm. DNA was then digested as described above for DNA containing reduced MTX-dR. LC/MS

grade H₂O was added for a final volume of 1 mL. MTX was enriched by SPE using the same conditions as reduced MTX-dR SPE enrichment, followed by vacuum centrifugation to dryness. The dried extracts were reconstituted in 10% CH₃CN 0.1% FA (250 µL), sonicated, and an aliquot of 2 µL diluted 1000-fold. The diluent was transferred into polypropylene autosampler vials for LC/MS³ analysis.

The MTX measurements were conducted on the same LC/MS system and the Advance CaptiveSpray source. A ProntoSIL C18AQ column (0.1 mm × 150 mm, 3 µm particle size, 100 Å pore size, NanoLCMS solutions, Gold River, CA) was used for chromatography. The mobile phase solvents were (A) 0.01% FA and (B) 95% acetonitrile containing 4.99% and 0.01% FA. The sample (2 µL) was injected onto the analytical column and the following elution gradient was applied: flow rate, 1 µL/min; isocratic at 1% B from 0 to 3 min; increased to 50% B at 13 min using a linear gradient; 50% to 99% B at 14 min; and held at 99% B from 12 to 14 min. Then, the percentage of the B solvent was reduced from 99 to 1% B over 1 min; and held at 1% B for 6 min for re-equilibration. The quantitation was conducted in the positive ion mode at the MS³ scan stage. The MS parameters were: the capillary temperature was 270 °C, the spray voltage was 2.0 kV, the S-lens RF level was 60%; normalized CID was 30%; injection time was 10 ms, the activation Q was 0.35 and 0.25, respectively, for MS² and MS³, and the isolation with *m/z* was set at 3.0 and 1.0 for MS² and MS³ scan stages. Quantitation was done in the positive ion mode. The MS³ transitions for MTX doubly charged species were 223.0 → 358.0 → 297.1, and the transition for [²H₈]-MTX was 227 → 362.0 → 297.1.

Calibration curves and limits of MTX-dR and MTX detection in CT DNA. Calibration curves were constructed for MTX-dR (**Figure S30**) and MTX (**Figure S31**) in a CT DNA digest matrix as follows: CT DNA (10 µg) was spiked with 50 pg MTX-[¹³C₅]dR (2.90 adducts

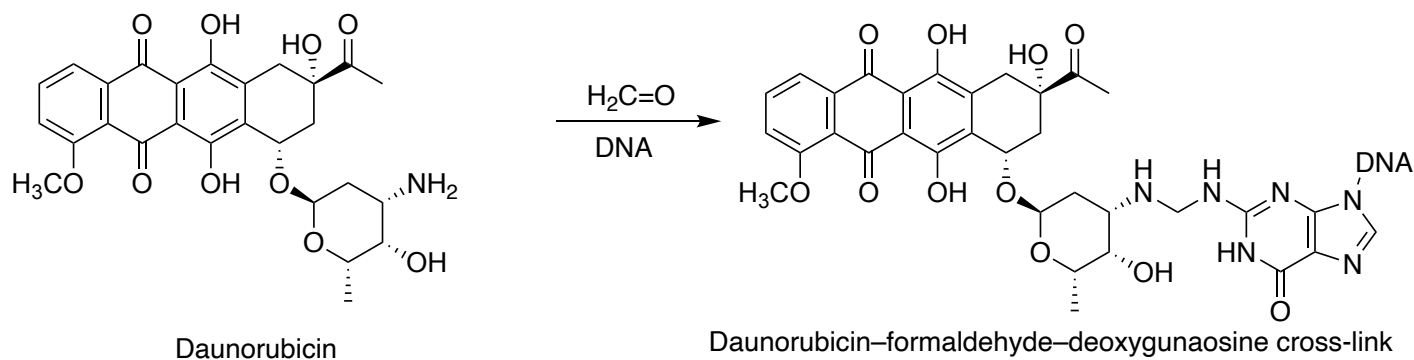
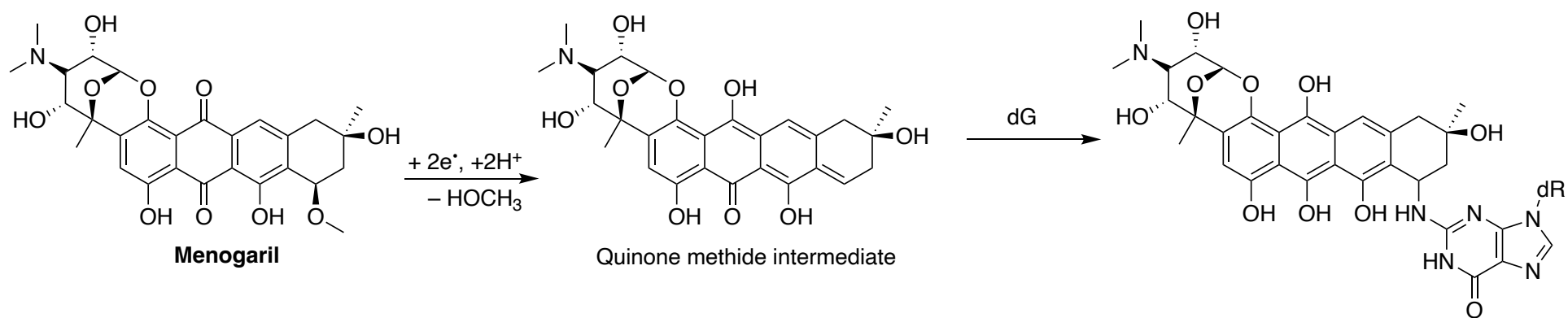
per 10^6 nts), and the MTX-dR standard was added at seven calibrant levels ranging from 0 to 4.83 MTX-dR adducts per 10^5 nts. The calibration curve for MTX was also constructed within a CT DNA digestion matrix. The DNA (10 μ g) DNA was spiked with 1.5 nmol [$^2\text{H}_8$]-MTX (0.68 μ g) and unlabeled MTX at seven calibrant levels ranging from 0, 0.1 to 30 nmol. The amount of [$^2\text{H}_8$]-MTX used as the calibrant was based on the estimated amount of MTX retained in the nuclear fraction (unpublished observations, M. Bellamri). The CT DNA samples of both calibration curves were enzymatically digested, and analytes were enriched by SPE according to protocol reported in Materials and Methods. Each calibration level was done in triplicate or quadruplicate, and the linear regression was done using ordinary least-squares with equal weightings. The goodness-of-fit regression value of $r^2 \geq 0.99$.

The intercept and standard error of the slope are reported and the following formula was used to estimate the limit of quantitation (LOQ) by the slope (S) of the regression and its standard deviation (σ): $\text{LOQ} = 10\sigma/S$.⁴ The LOQ value for MTX-dR was estimated at 3.0 adducts per 10^7 nts. The LOQ for MTX uptake in nuclei was estimated at 187 pg per 10 μ g of DNA, which corresponds to 0.042 pmol MTX per μ g of DNA assuming 10 μ g of DNA per million MDA-MB-231 cells. The reported LOQ for MTX uptake is underestimated because the signal was obtained from a 1000-fold dilution of the nuclear matrix after solid-phase extraction (SPE) (Supporting Information). The LOQ for AP sites measured as their O-(pyridin-3-ylmethyl)hydroxylamine (PMOA-dR) derivative was previously determined as 1.6 AP sites per 10^8 nts in 10 μ g of enzymatically digested CT DNA serving as the background matrix.³ The levels of MTX-dR and AP sites, and MTX uptake in cells exceeded their LOQ values.

Statistics. Statistics on targeted analytes and other endpoints were performed with Prism 8.4.3 (GraphPad Software, La Jolla, CA). The statistical significance effect of treatment within a group was determined by the Student's *t*-test or two-way ANOVA. The data are reported as the mean \pm SD or mean \pm SEM * $P < 0.05$; ** $P < 0.01$, *** $P < 0.005$, **** $P < 0.001$ versus control). All studies were performed with at least three independent experiments in triplicate.

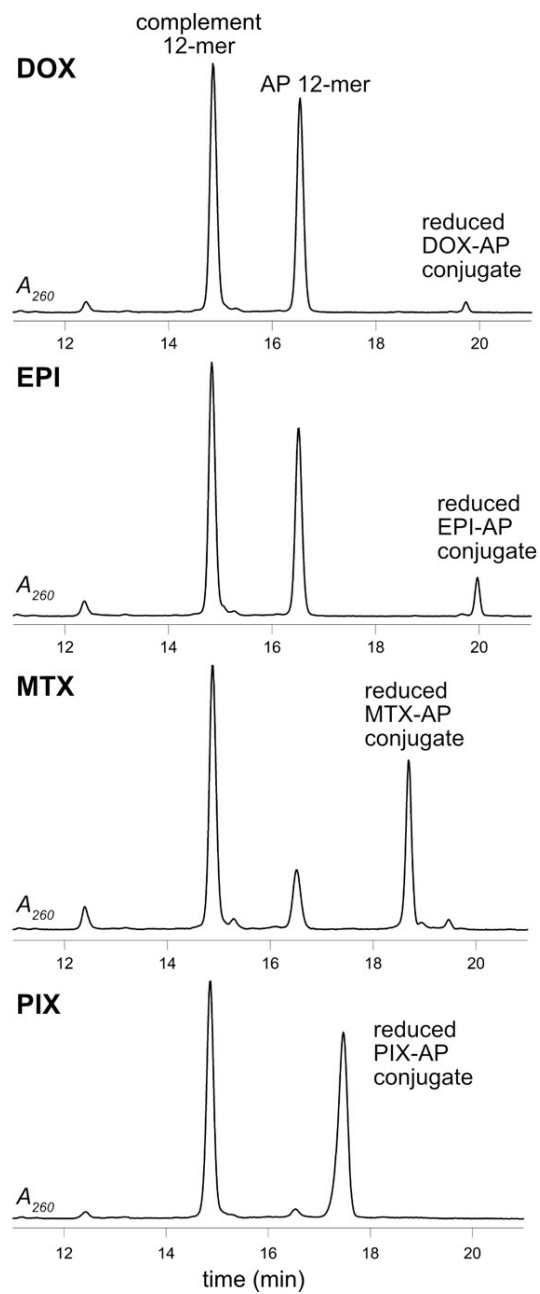
References

- (1) McLuckey, S. A.; Van Berkel, G. J.; Glish, G. L. Tandem mass spectrometry of small, multiply charged oligonucleotides. *J Am Soc Mass Spectrom* **1992**, 3 (1), 60-70. DOI: 10.1016/1044-0305(92)85019-G From NLM PubMed-not-MEDLINE.
- (2) Christov, P. P.; Son, K. J.; Rizzo, C. J. Synthesis and characterization of oligonucleotides containing a nitrogen mustard formamidopyrimidine monoadduct of deoxyguanosine. *Chem Res Toxicol* **2014**, 27 (9), 1610-1618. DOI: 10.1021/tx5002354 From NLM Medline.
- (3) Chen, H.; Yao, L.; Brown, C.; Rizzo, C. J.; Turesky, R. J. Quantitation of apurinic/apyrimidinic sites in isolated DNA and in mammalian tissue with a reduced level of artifacts. *Anal. Chem.* **2019**, 91 (11), 7403-7410. DOI: 10.1021/acs.analchem.9b01351.
- (4) Guidance for Industry, Bioanalytical Method Validation, U.S. Department of Health and Human Services, Food and Drug Administration, Center for Drug Evaluation and Research (CDER), Center for Veterinary Medicine (CMV), May 2018. Document available at <https://www.fda.gov/downloads/drugs/guidances/ucm070107.pdf>.



Scheme S1. Previously proposed mechanisms of covalent modification of DNA by anthracyclines. Top: Reductive activation of Menogaril to its quinone methide and its subsequent reaction with dG. Bottom: Formation of a dG-formaldehyde-doxorubicin covalent conjugate.

6 hrs



24 hrs

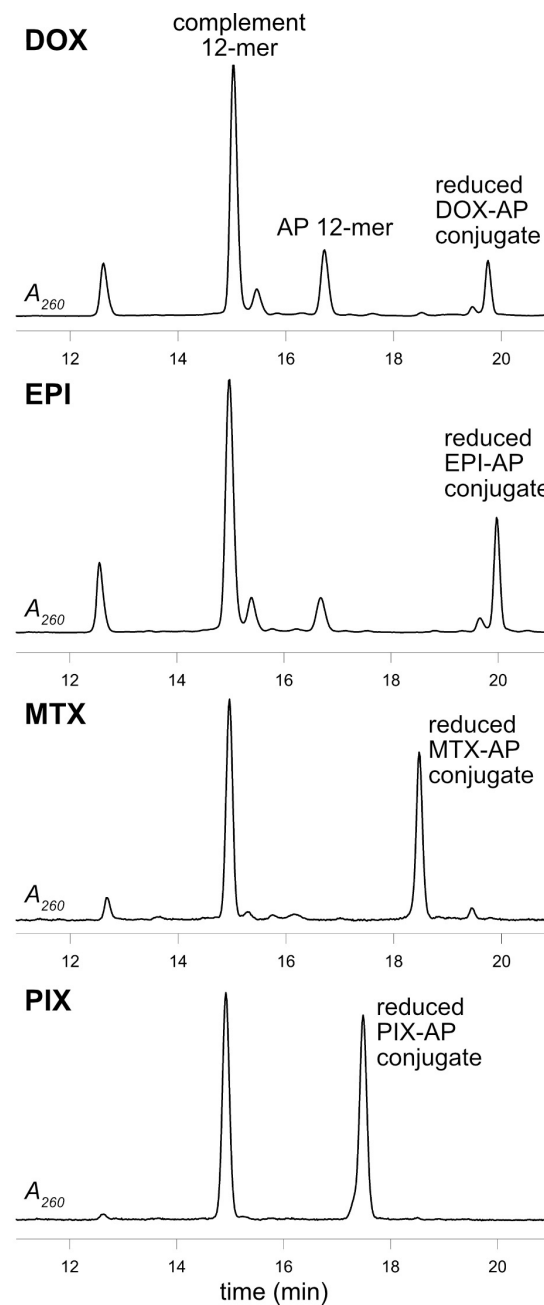


Figure S1. HPLC chromatograms of the reaction of the AP-containing 12-mer duplex (5'-GTT GCN CGT ATG-3') with DOX, EPI, MTX, and PIX reduced with $\text{NaB}(\text{CN})\text{H}_3$ analyzed after 6 (left) and 24 (right) hrs.

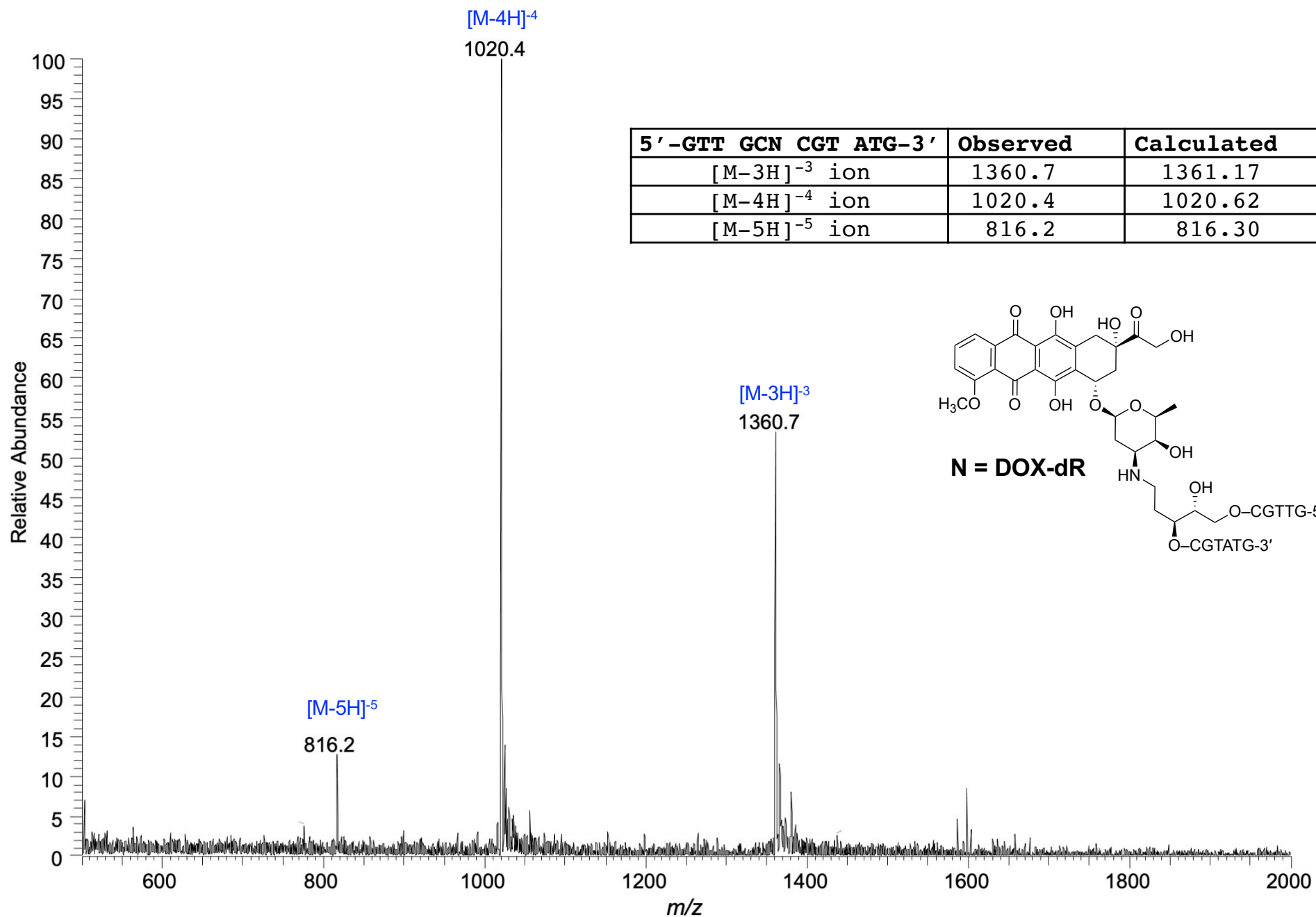


Figure S2. Mass spectrum of 5'-GTT GCN CGT ATG-3' where N is the reduced DOX-dR conjugate.

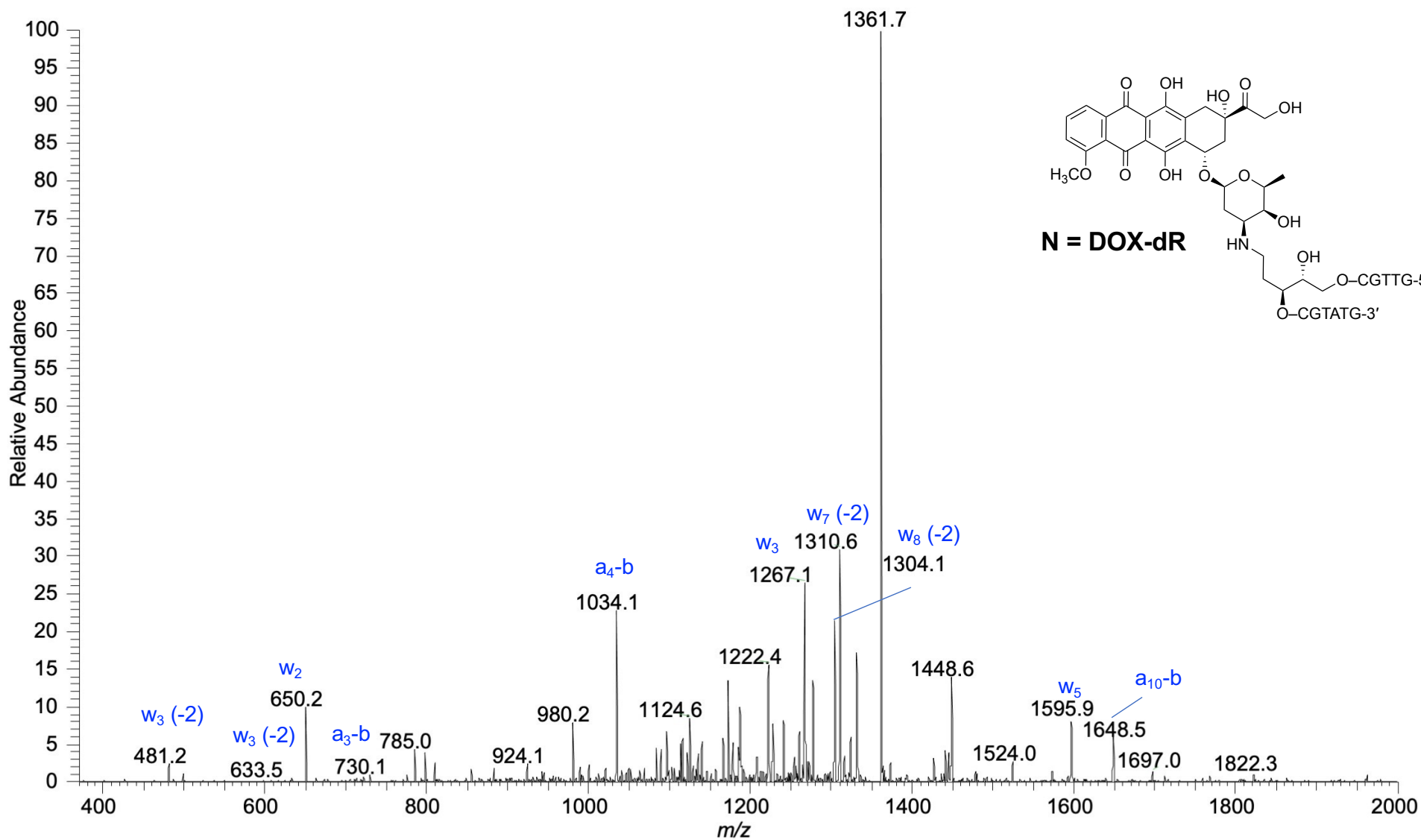


Figure S3. CID mass spectrum of the m/z 1360.9 (-3) ion of 5'-GTT GCN CGT ATG-3' where N is the reduced DOX-dR conjugate. See Figure S40 for fragment ion nomenclature.

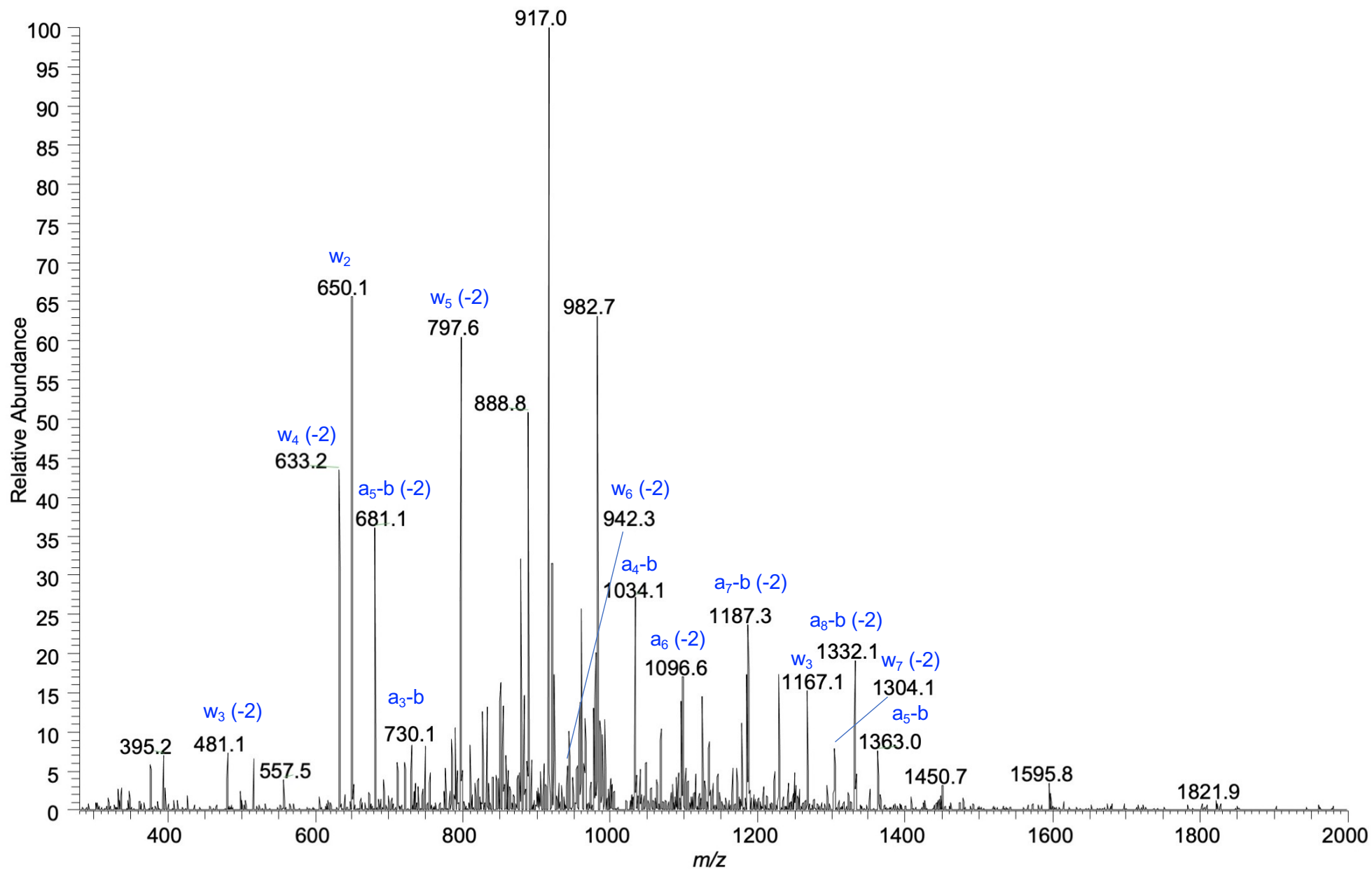


Figure S4. CID mass spectrum of the m/z 1020.5 (-4) ion of 5'-GTT GCN CGT ATG-3' where N is the reduced DOX-dR conjugate.

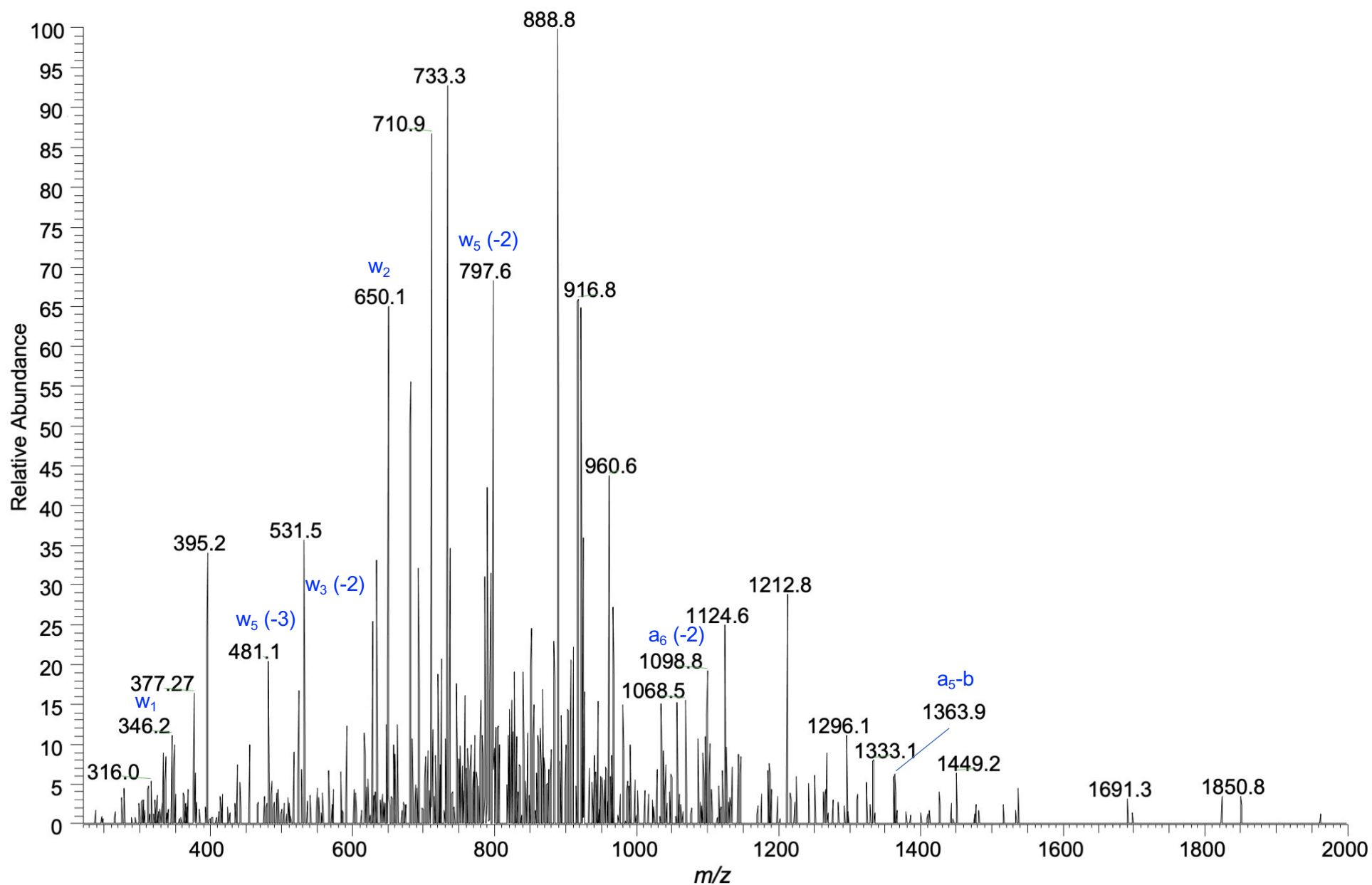


Figure S5. CID mass spectrum of the m/z 816.2 (-5) ion of 5'-GTT GCN CGT ATG-3' where N is the reduced DOX-dR conjugate.

5' -GTT GCN CGT ATG-3'	Ion	Observed	Calculated
5' -GT	a ₃ -b	730.1 ^{1,2}	730.13
5' -GTT	a ₄ -b	1034.1 ^{1,2}	1034.17
5' -GTT G	a ₅ -b	1363.0 ²	1363.22
	a ₅ -b (-2)	681.1 ²	681.11
5' -GTT GCN	a ₆ (-2)	1098.5 ^{2,3}	1097.72
5' -GTT GCN	a ₇ -b (-2)	1187.3 ^{1,2}	1187.23
5' -GTT GCN C	a ₈ -b (-2)	1332.1 ¹	1331.66
5' -GTT GCN CGT A	a ₁₀ -b (-2)	1648.5 ¹	1648.30
CN CGT ATG-3'	w ₈ (-2)	1448.5 ¹	1448.27
N CGT ATG-3'	w ₇ (-2)	1304.1 ^{1,2}	1303.75
CGT ATG-3'	w ₆ (-2)	942.3 ²	942.15
GT ATG-3'	w ₅	1595.8 ¹	1596.26
	w ₅ (-2)	797.6 ^{1,2}	797.62
T ATG-3'	w ₄	1267.1 ^{1,2}	1267.20
	w ₄ (-2)	633.2 ²	633.10
ATG-3'	w ₃ (-2)	481.2 ^{1,2}	481.07
TG-3'	w ₂	650.1 ^{1,2}	650.10

N = DOX-dR

¹ ion observed from the CID spectrum of the 1360.9 (-3) parent ion

² ion observed from the CID spectrum of the 1020.5 (-4) parent ion

³ ion observed from the CID spectrum of the 816.2 (-5) parent ion

Table S1. CID fragment ions from 5'-GTT GCN CGT ATG-3' where N is the reduced DOX-dR conjugate.

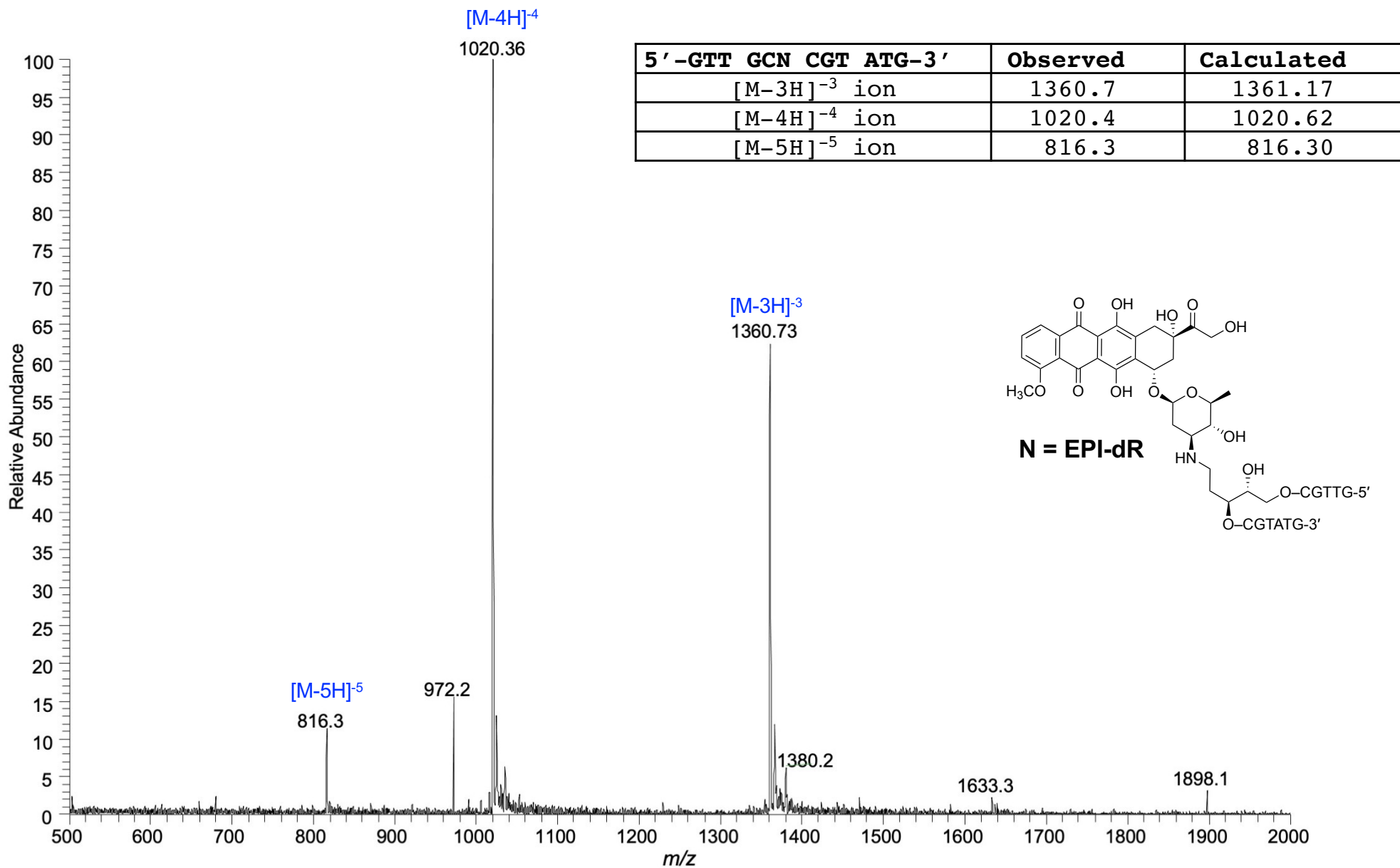


Figure S6. Mass spectrum of 5'-GTT GCN CGT ATG-3' where N is the reduced EPI-dR conjugate.

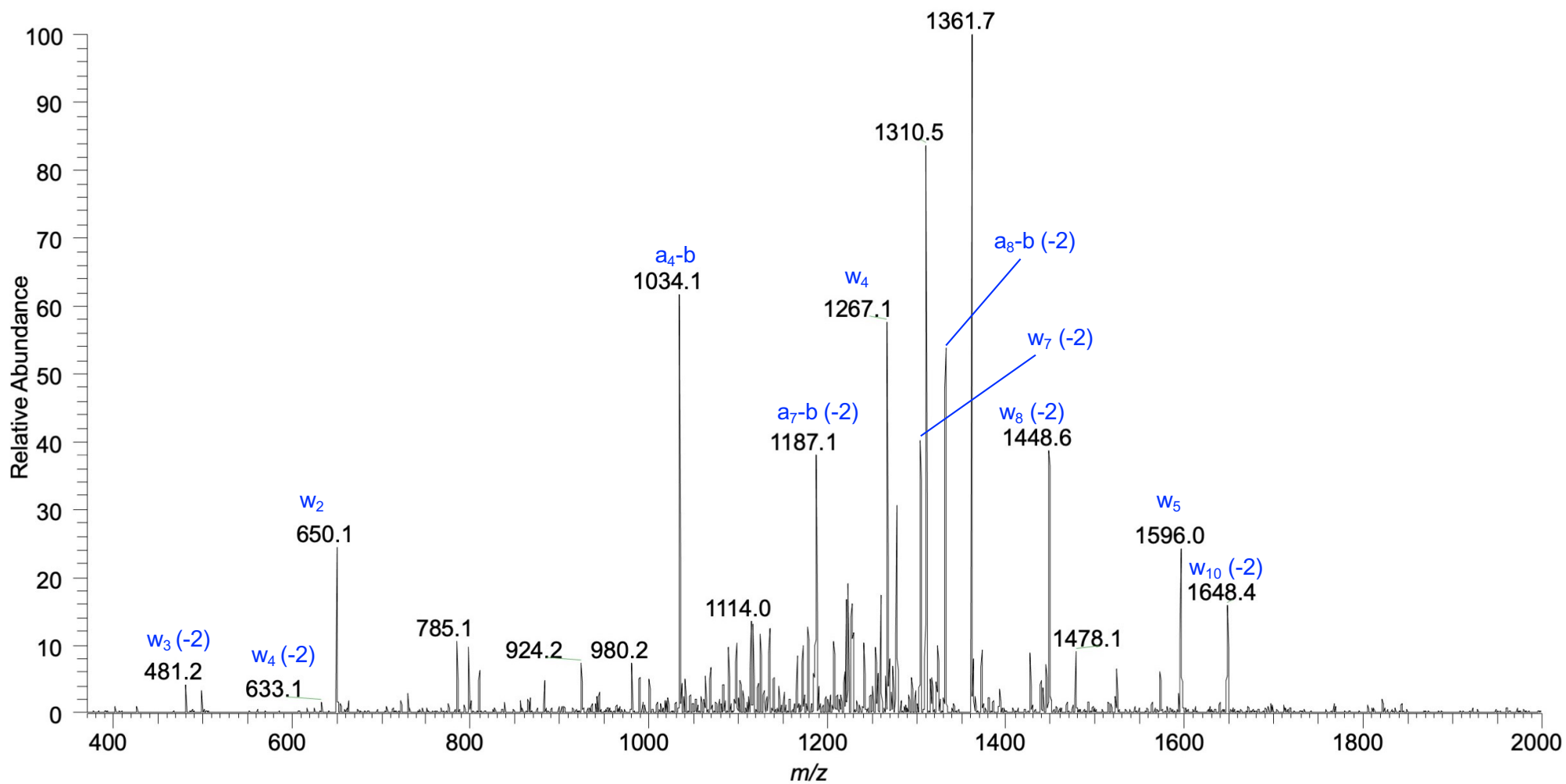


Figure S7. CID mass spectrum of the m/z 1360.9 (-3) ion of 5'-GTT GCN CGT ATG-3' where N is the reduced EPI-dR conjugate.

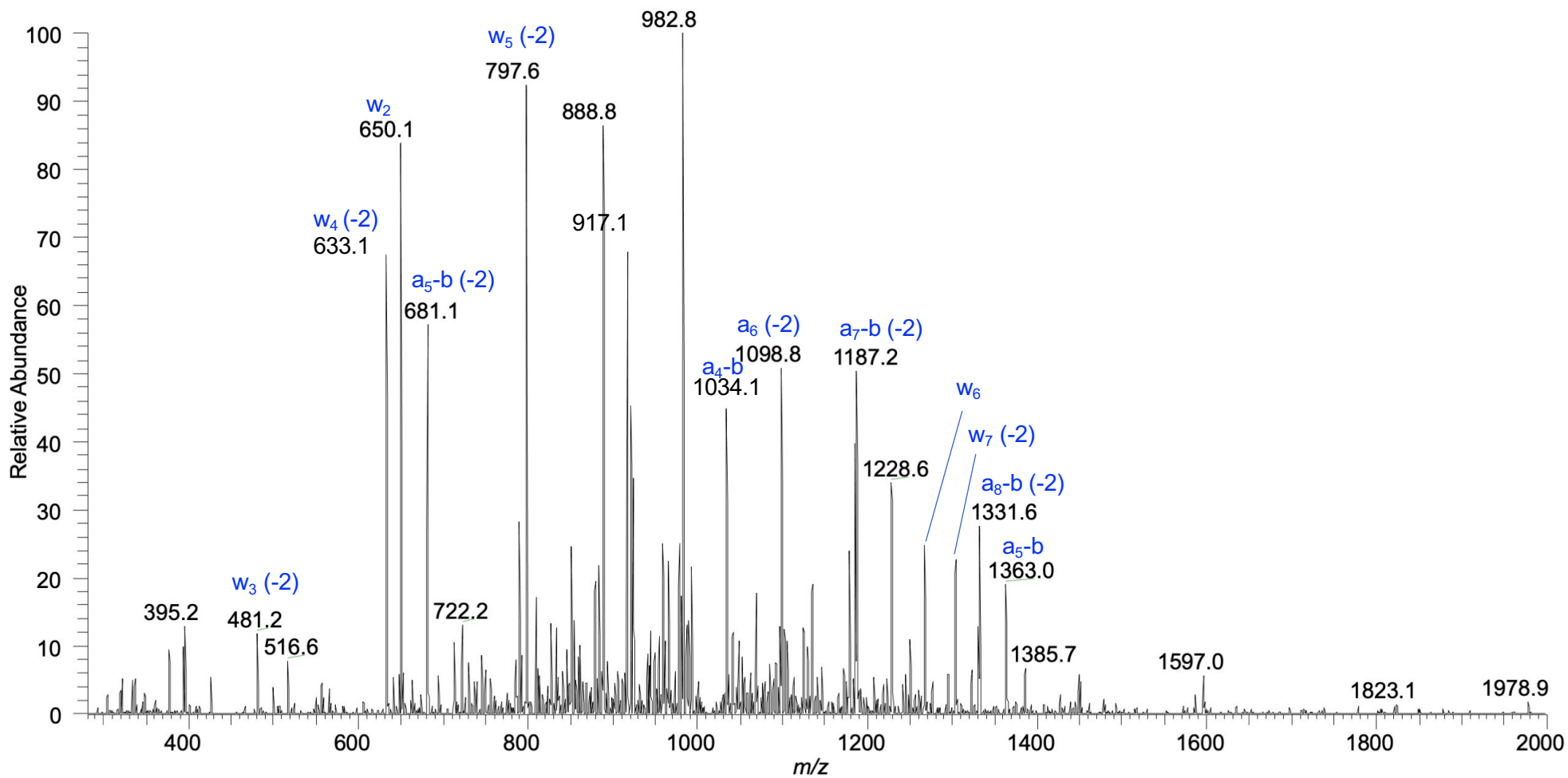


Figure S8. CID mass spectrum of the m/z 1020.5 (-4) ion of 5'-GTT GCN CGT ATG-3' where N is the reduced EPI-dR conjugate.

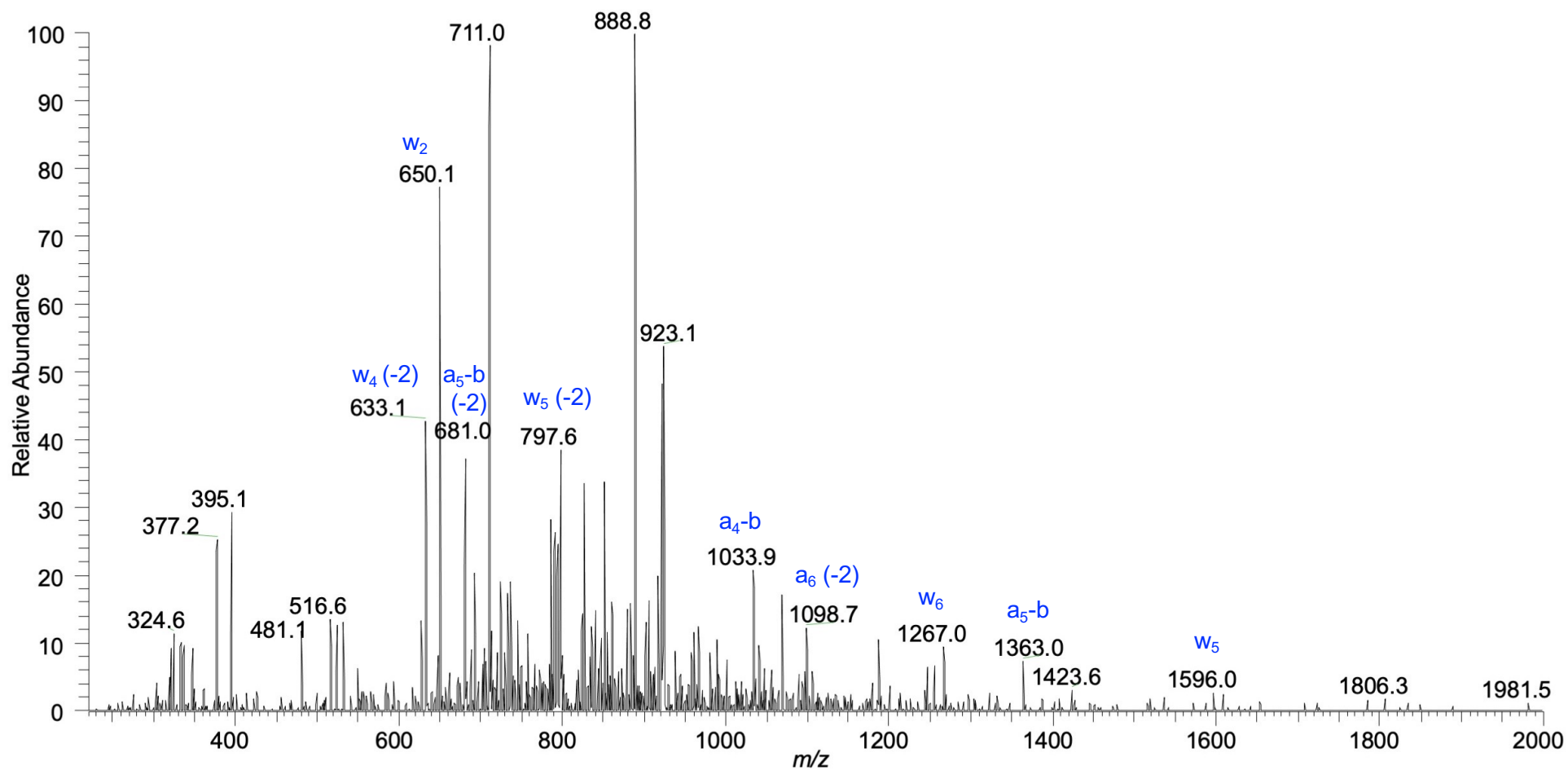


Figure S9. CID mass spectrum of the m/z 816.2 (-5) ion of 5'-GTT GCN CGT ATG-3' where N is the reduced EPI-dR conjugate.

5'-GTT GCN CGT ATG-3'	Ion	Observed	Calculated
5'-GTT	a ₄ -b	1034.1 ^{1,2}	1034.17
5'-GTT G	a ₅ -b	1363.0 ²	1363.22
	a ₅ -b (-2)	681.1 ²	681.11
5'-GTT GCN	a ₆	1098.8 ²	1097.72
5'-GTT GCN	a ₇ -b (-2)	1187.1 ^{1,2}	1187.23
5'-GTT GCN C	a ₈ -b (-2)	1331.7 ¹	1331.66
5'-GTT GCN CGT A	a ₁₀ -b (-2)	1648.4 ¹	1648.30
CN CGT ATG-3'	w ₈ (-2)	1448.6 ^{1,2}	1448.27
N CGT ATG-3'	w ₇ (-2)	1303.6 ^{1,2}	1303.75
GT ATG-3'	w ₅	1596.0 ¹	1596.26
	w ₅ (-2)	797.6 ²	797.62
T ATG-3'	w ₄	1267.1 ^{1,2}	1267.20
	w ₄ (-2)	633.1 ^{1,2}	633.10
ATG-3'	w ₃ (-2)	481.1 ^{1,2}	481.07
TG-3'	w ₂	650.1 ^{1,2}	650.10

N = EPI-dR

¹ ion observed from the CID spectrum of the 1360.9 parent ion

² ion observed from the CID spectrum of the 1020.5 parent ion

Table S2. CID fragment ions from 5'-GTT GCN CGT ATG-3' where N is the reduced EPI-dR conjugate.

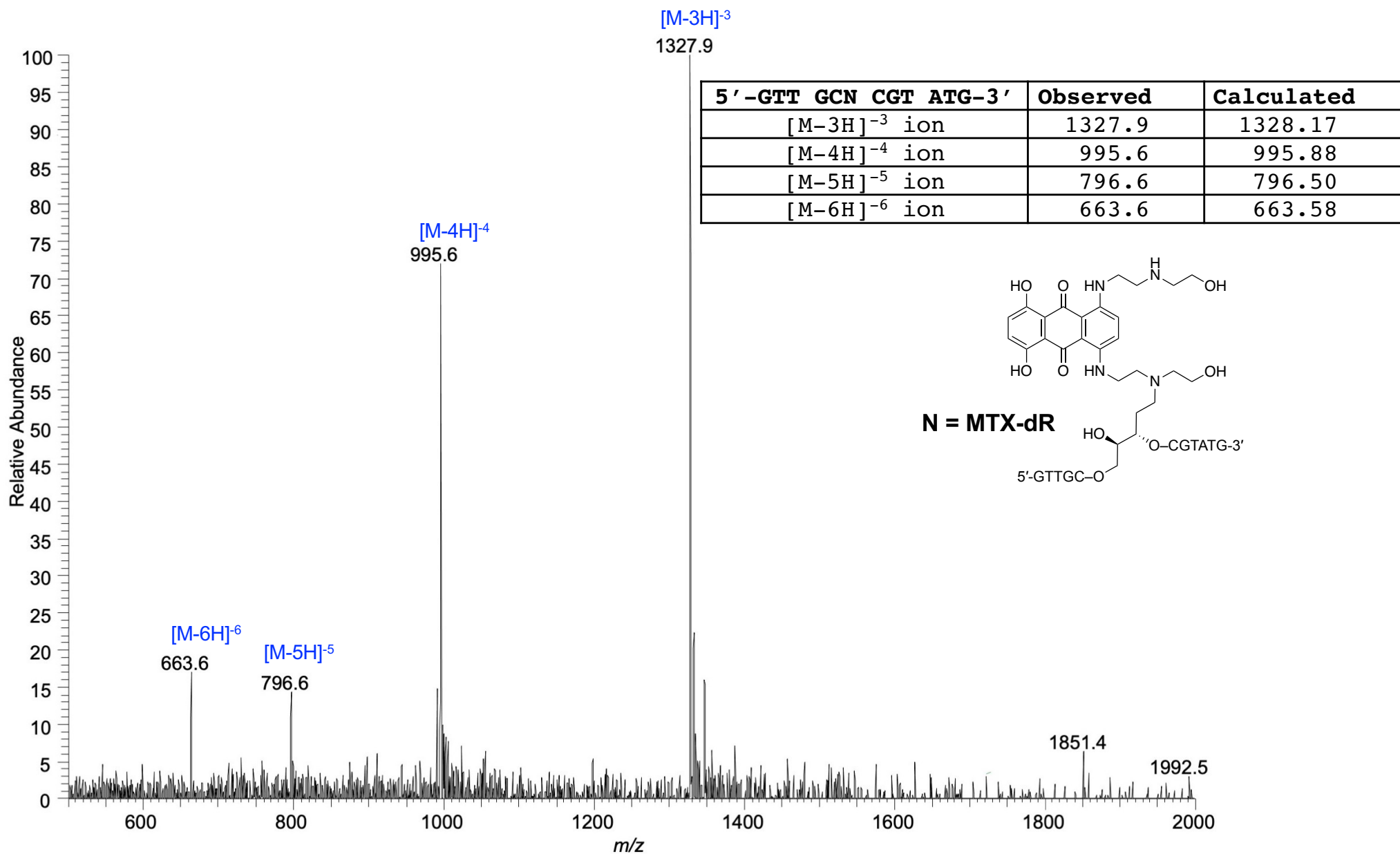


Figure S10. Mass spectrum of 5'-GTT GCN CGT ATG-3' where N is the reduced MTX-dR conjugate.

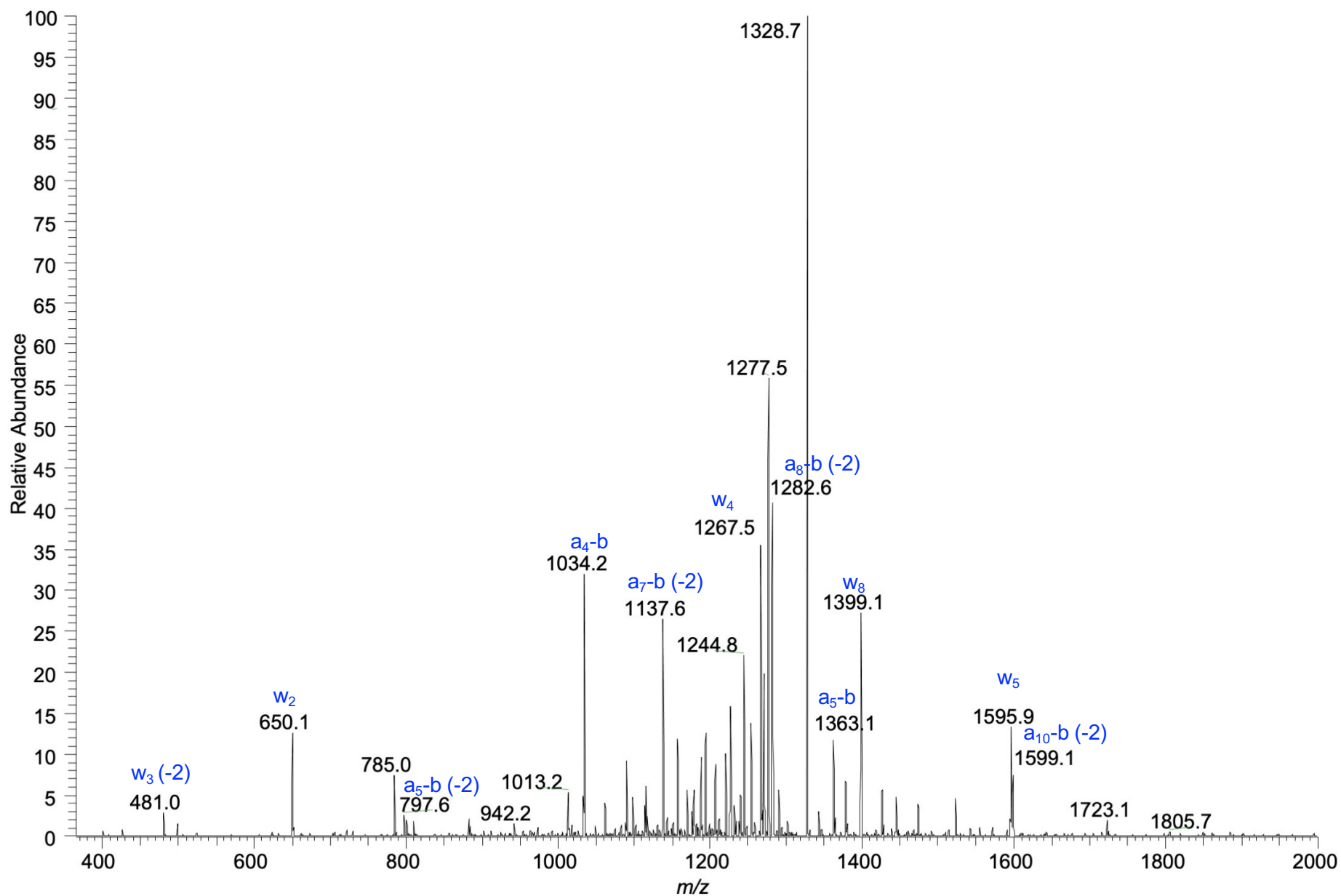


Figure S11. CID mass spectrum of the m/z 1327.9 (-3) ion of 5'-GTT GCN CGT ATG-3' where N is the reduced MTX-dR conjugate.

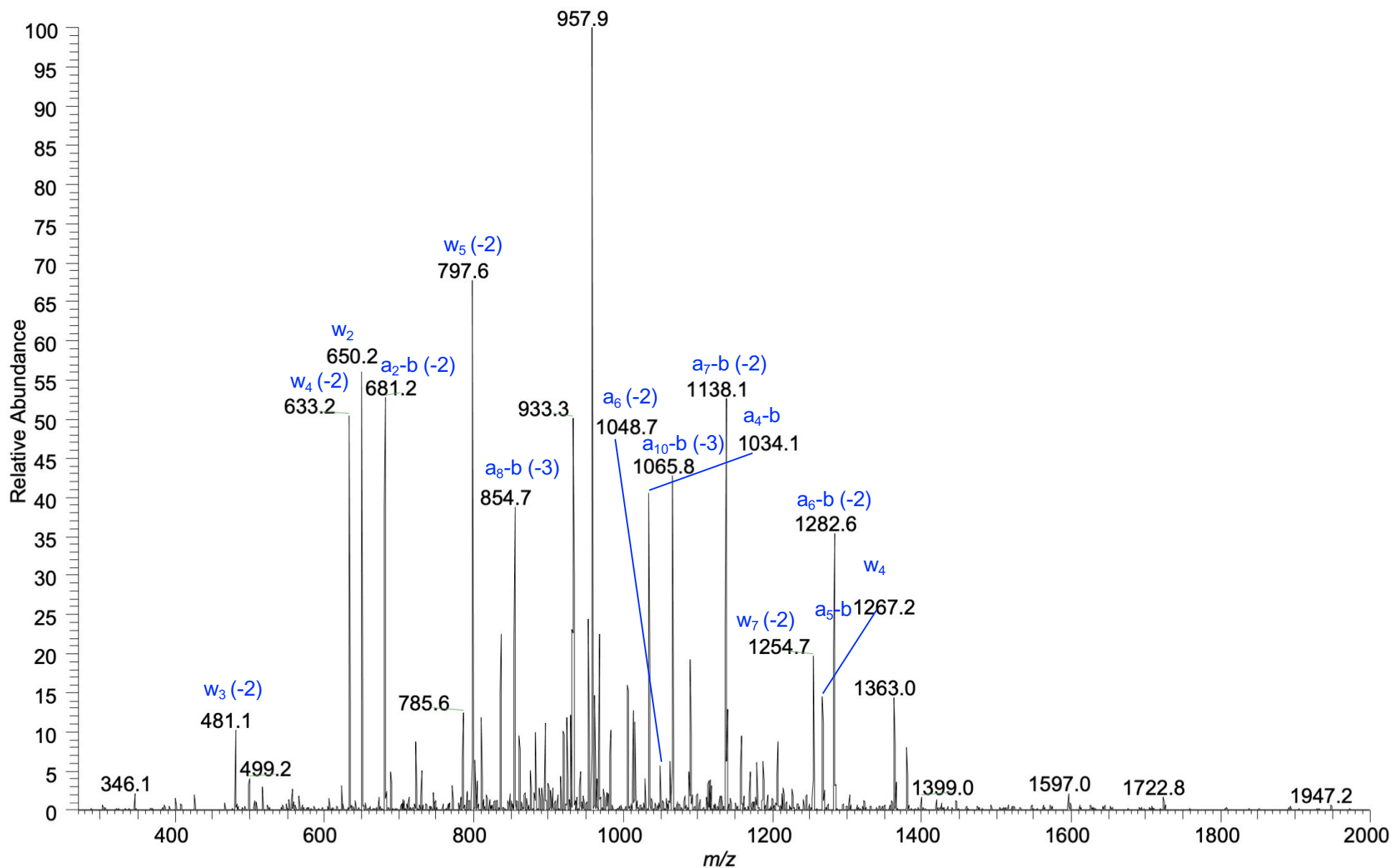


Figure S12. CID mass spectrum of the m/z 796.4 (-5) ion of 5'-GTT GCN CGT ATG-3' where N is the reduced MTX-dR conjugate.

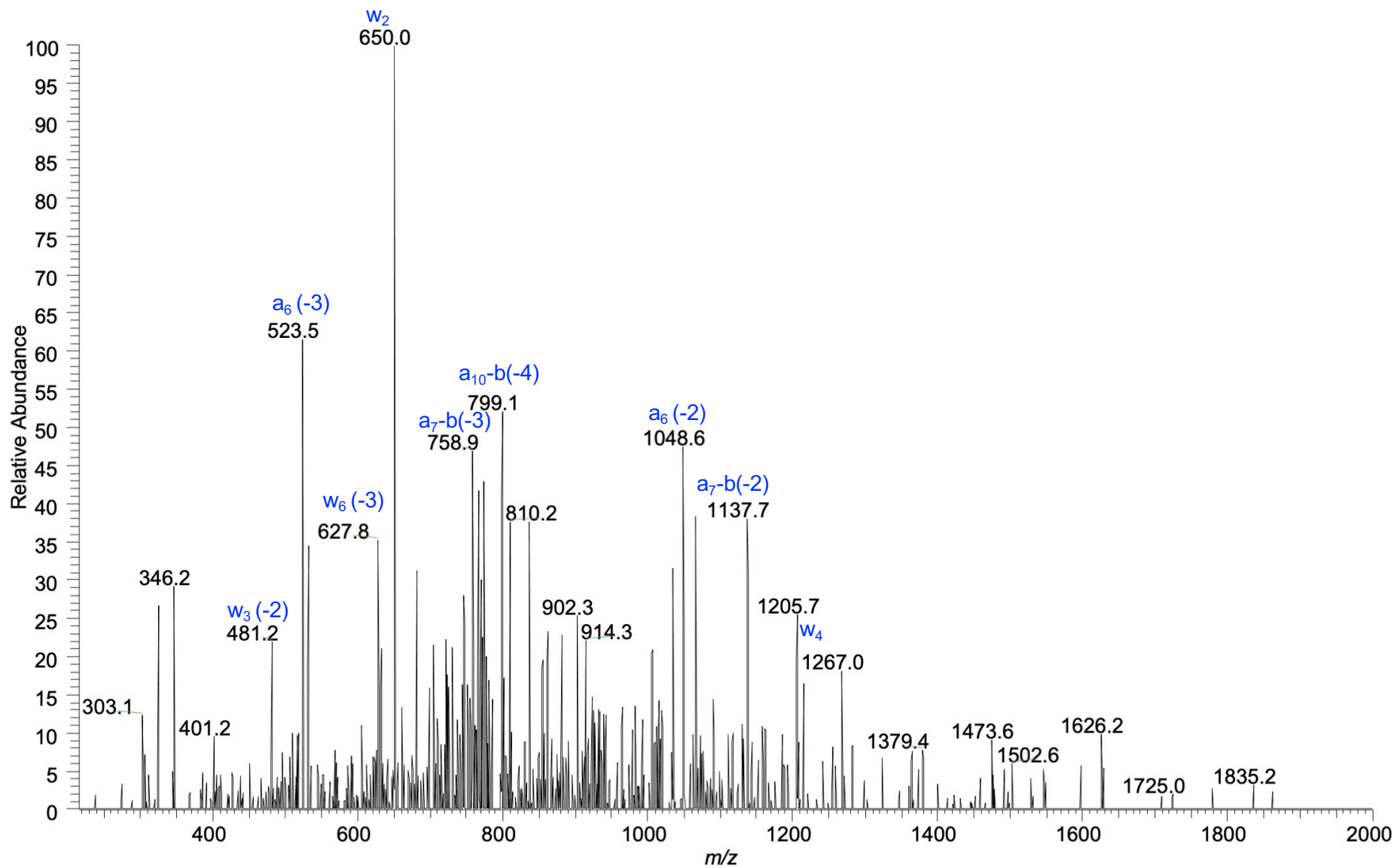


Figure S13. CID mass spectrum of the m/z 995.6 (-4) ion of 5'-GTT GCN CGT ATG-3' where N is the reduced MTX-dR conjugate.

5' -GTT GCN CGT ATG-3'	Ion	Observed	Calculated
5' -GTT	a ₄ -b	1034.1 ^{1,2}	1034.17
5' -GTT G	a ₅ -b	1363.1 ²	1363.22
	a ₅ -b (-2)	681.1 ²	681.11
5' -GTT GCN	a ₆	1048.7 ^{2,3}	1048.24
5' -GTT GCN	a ₇ -b (-2)	1138.1 ^{2,3}	1137.74
5' -GTT GCN C	a ₈ -b (-2)	1282.6 ^{1,2}	1282.26
5' -GTT GCN CGT A	a ₁₀ -b (-2)	1599.1 ¹	1598.81
CN CGT ATG-3'	w ₈ (-2)	1399.1 ¹	1398.78
N CGT ATG-3'	w ₇ (-2)	1304.7 ^{1,2}	1254.26
GT ATG-3'	w ₅	1595.9 ¹	1596.26
	w ₅ (-2)	797.6 ²	797.62
T ATG-3'	w ₄	1267.5 ^{1,2}	1267.20
	w ₄ (-2)	633.2 ²	633.10
ATG-3'	w ₃ (-2)	481.0 ^{1,2}	481.07
TG-3'	w ₂	650.1 ^{1,2}	650.10

N = MTX-dR

¹ ion observed from the CID spectrum of the 1327.9 (-3) parent ion

² ion observed from the CID spectrum of the 995.6 (-4) parent ion

³ ion observed from the CID spectrum of the 796.6 (-5) parent ion

Table S3. CID fragment ions from 5'-GTT GCN CGT ATG-3' where N is the reduced EPI-dR conjugate.

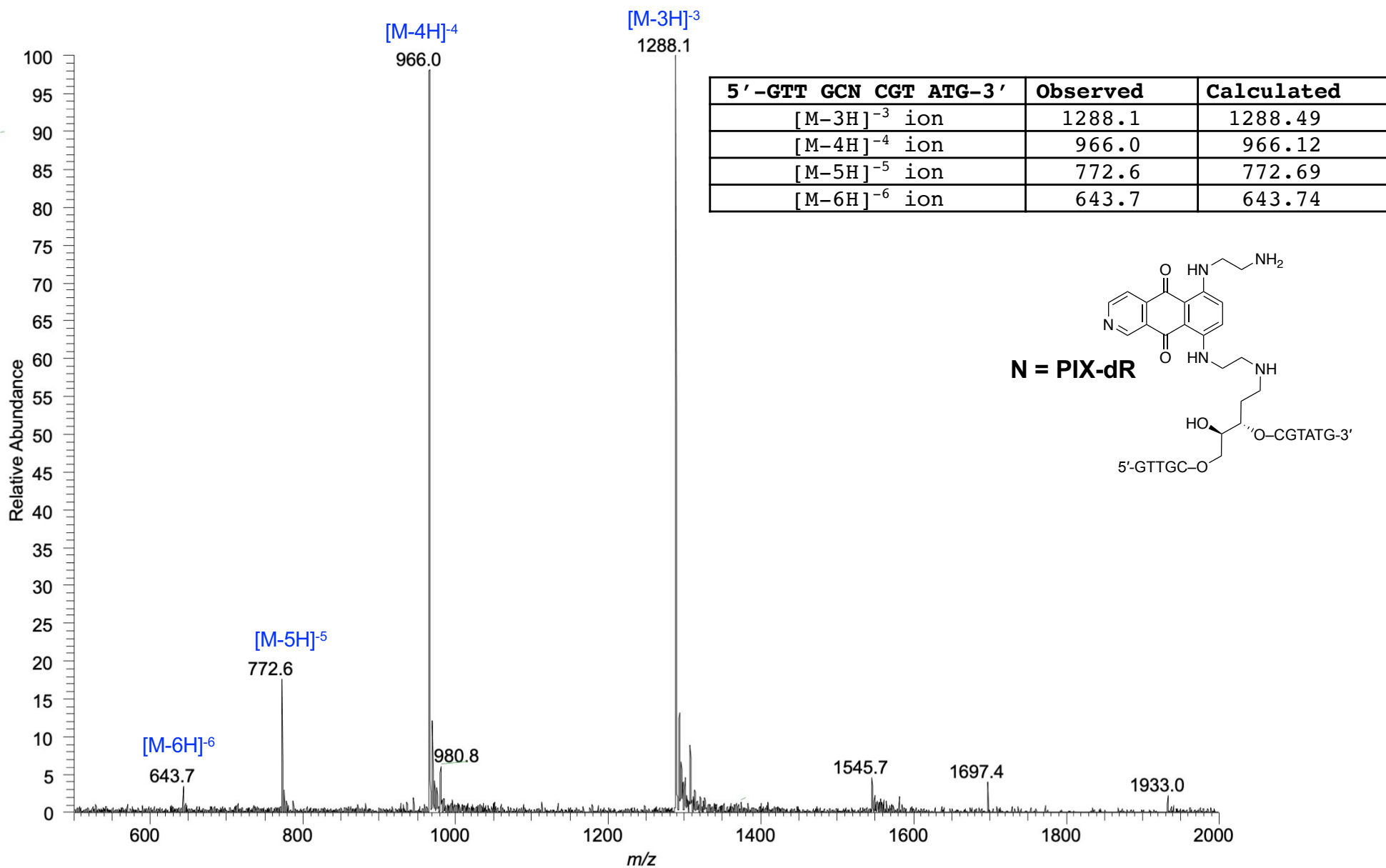


Figure S14. Mass spectrum of 5'-GTT GCN CGT ATG-3' where N is the reduced PIX-dR conjugate.

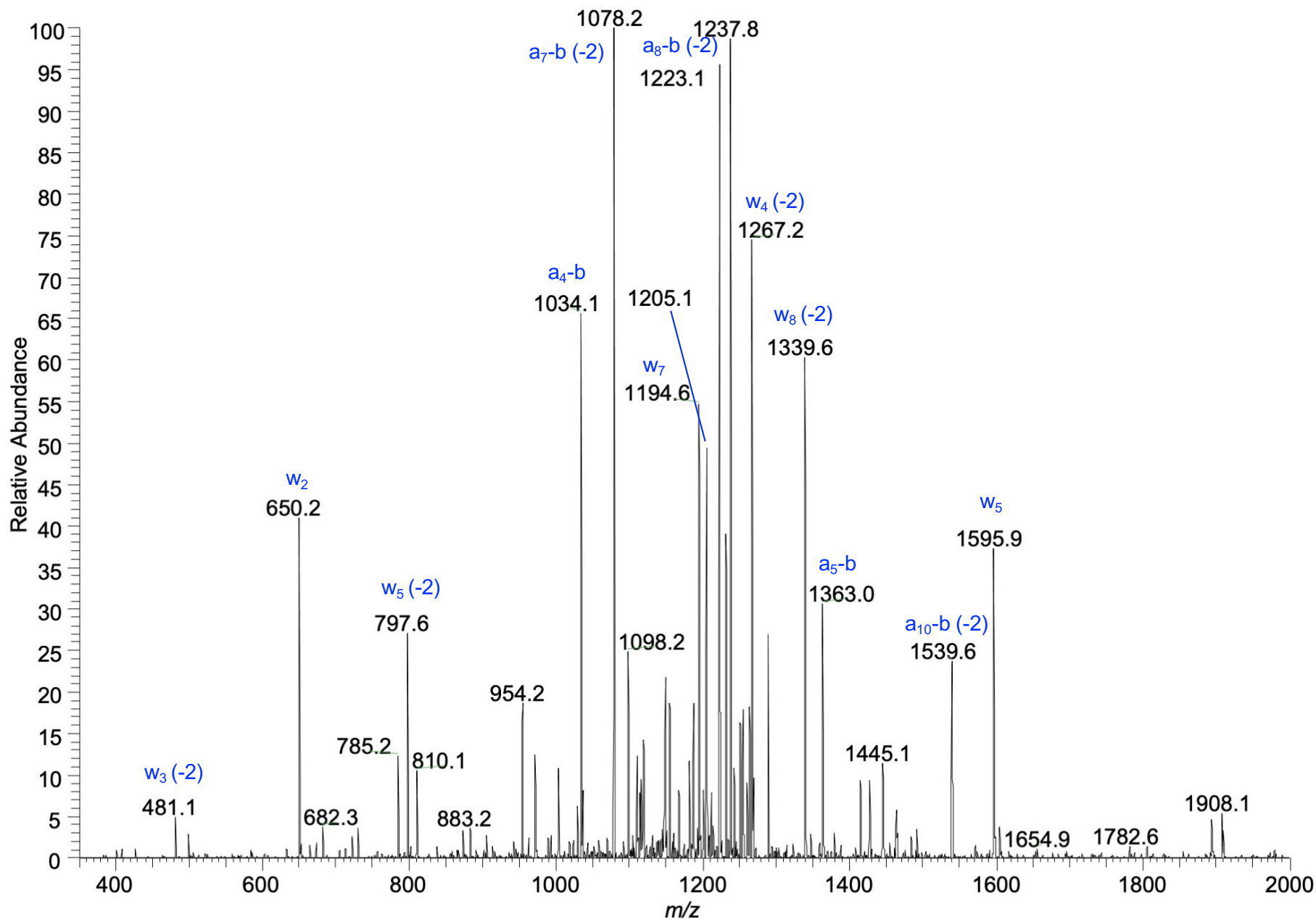


Figure S15. CID mass spectrum of the m/z 1288.1 (-3) ion of 5'-GTT GCN CGT ATG-3' where N is the reduced PIX-dR conjugate.

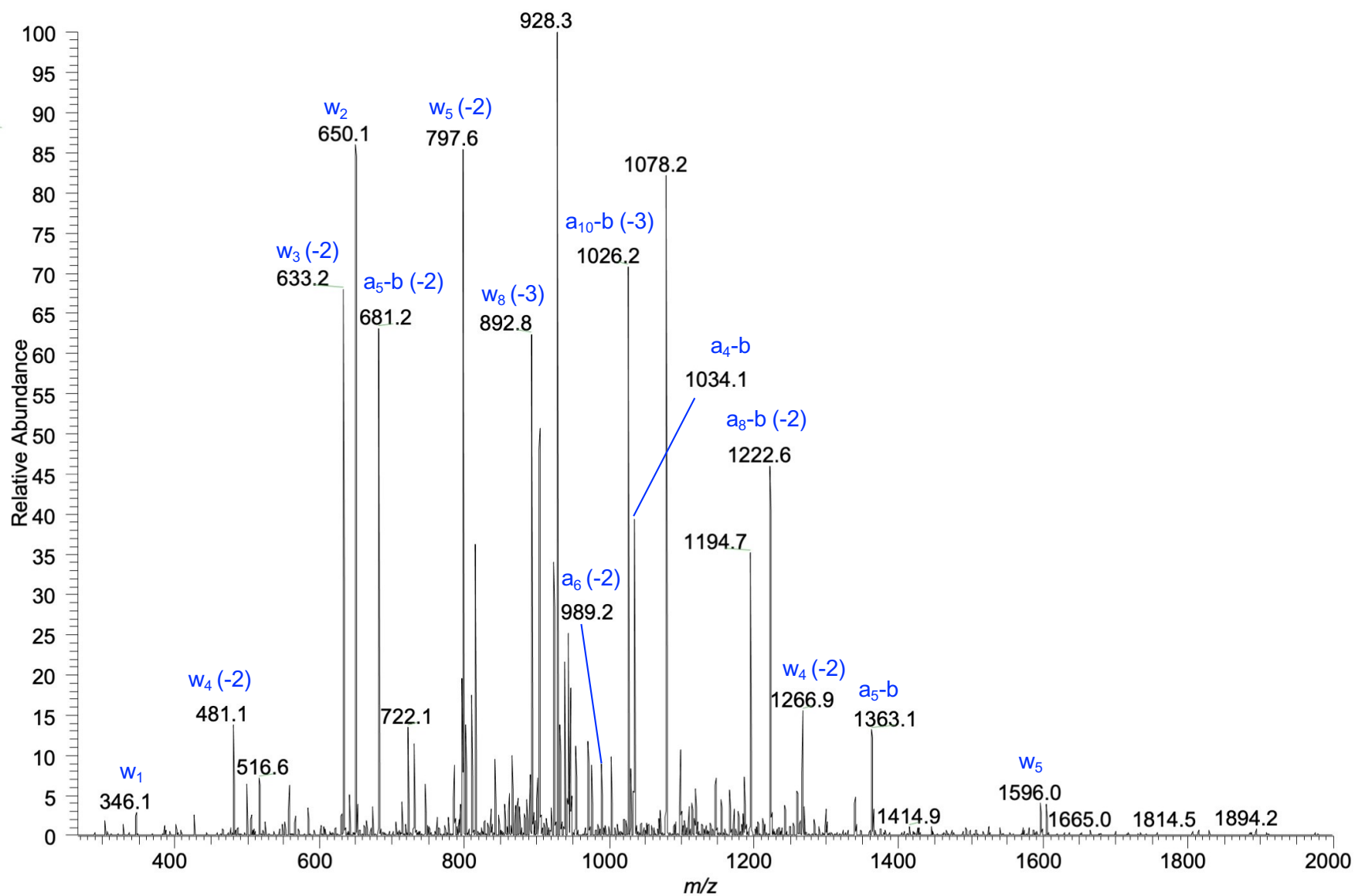


Figure S16. CID mass spectrum of the m/z 966.0 (-4) ion of 5'-GTT GCN CGT ATG-3' where N is the reduced MTX-dR conjugate.

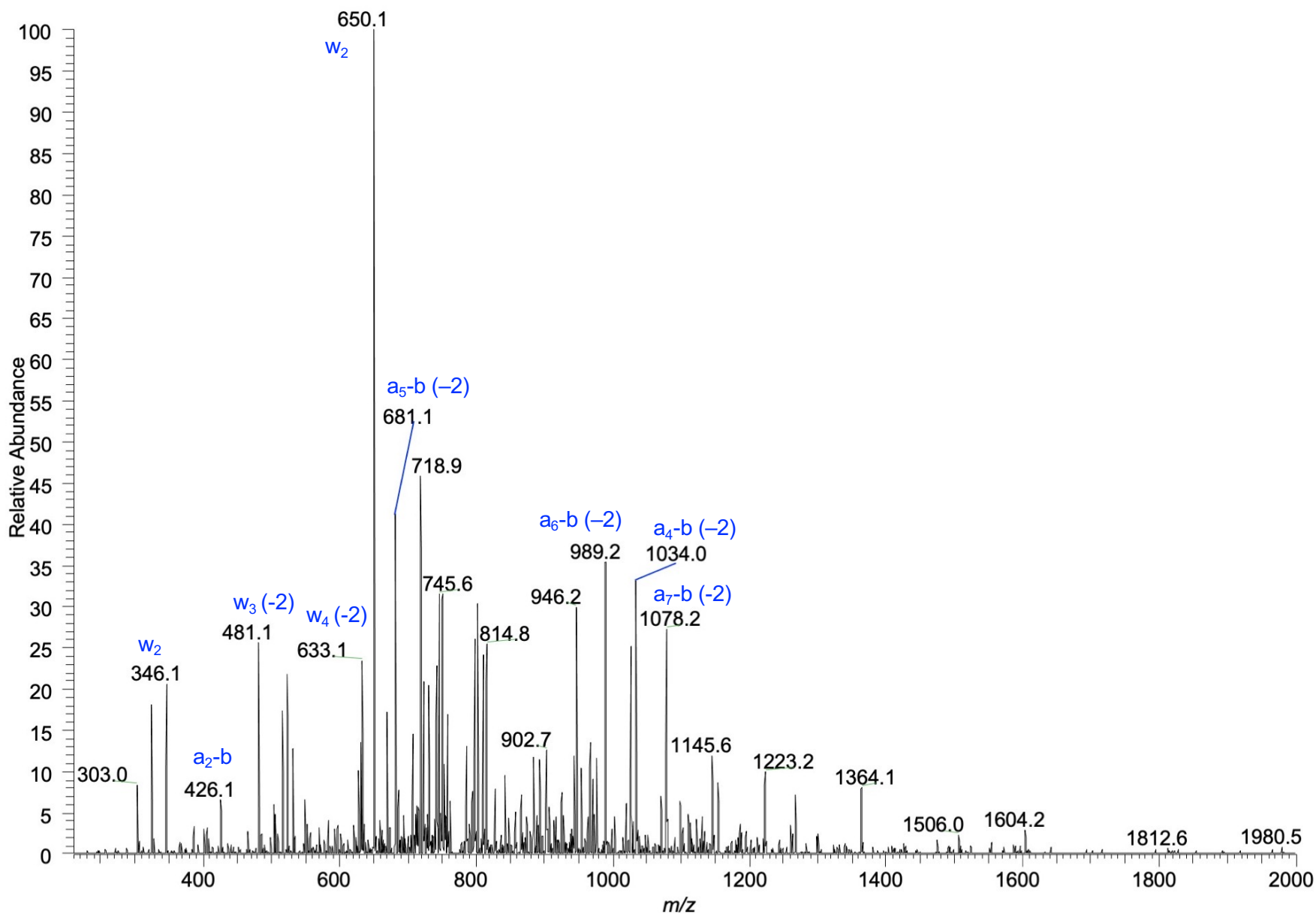


Figure S17. CID mass spectrum of the m/z 722.6 (-5) ion of 5'-GTT GCN CGT ATG-3' where N is the reduced PIX-dR conjugate.

5'-GTT GCN CGT ATG-3'	Ion	Observed	Calculated
5'-GTT	a ₄ -b	1034.1 ^{1,2}	1034.17
5'-GTT G	a ₅ -b	1363.0 ²	1363.22
	a ₅ -b (-2)	681.2 ^{2,3}	681.11
5'-GTT GCN	a ₆ (-2)	989.2 ²	988.72
5'-GTT GCN	a ₇ -b (-2)	1078.2 ^{1,2,3}	1078.22
5'-GTT GCN C	a ₈ -b (-2)	1222.6 ²	1222.74
5'-GTT GCN CGT A	a ₁₀ -b (-2)	1539.6 ¹	1539.29
CN CGT ATG-3'	w ₈ (-2)	1339.6 ¹	1339.26
	w ₈ (-3)	892.8 ²	892.50
N CGT ATG-3'	w ₇ (-2)	1194.6 ¹	1194.74
GT ATG-3'	w ₅	1595.9 ^{1,2}	1596.26
	w ₅ (-2)	797.6 ^{1,2}	797.62
T ATG-3'	w ₄	1267.1 ^{1,2}	1267.20
	w ₄ (-2)	633.2 ^{2,3}	633.10
ATG-3'	w ₃ (-2)	481.1 ^{1,2,3}	481.07
TG-3'	w ₂	650.1 ^{1,2,3}	650.10
G-3'	w ₁	346.1 ^{2,3}	346.05

N = PIX-dR

¹ ion observed from the CID spectrum of the 1288.1 (-3) parent ion

² ion observed from the CID spectrum of the 966.0 (-4) parent ion

³ ion observed from the CID spectrum of the 722.6 (-5) parent ion

Table S4. CID fragment ions from 5'-GTT GCN CGT ATG-3' where N is the reduced PIX-dR conjugate.

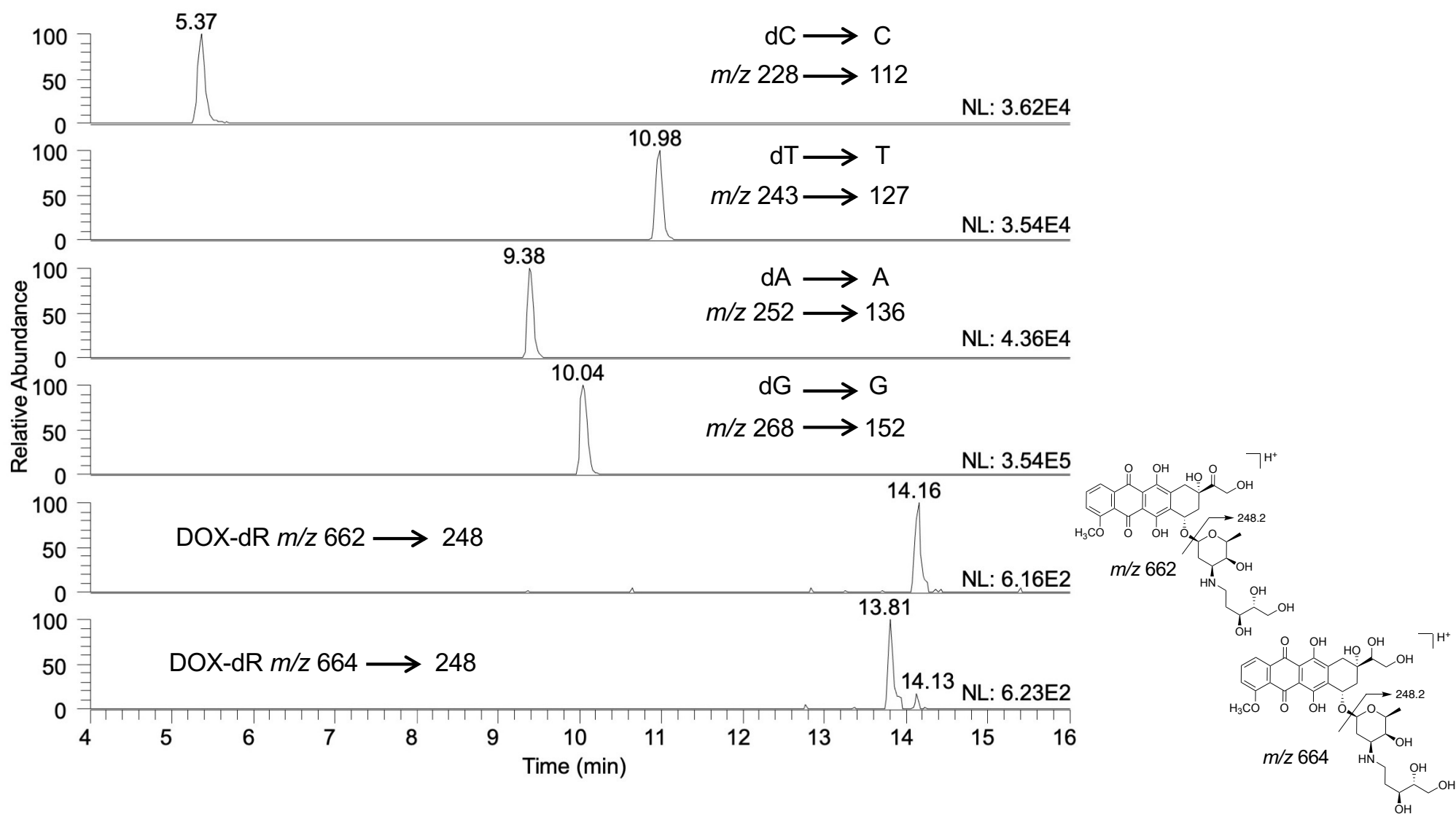


Figure S18. Extracted ion chromatograms of the enzymatic digestion of the reduced DOX-dR containing 12-mer oligonucleotide (5'-GTT GCN CGT ATG-3'). Ion trap CID was employed at the MS² scan stage to follow the loss of deoxyribose (−116 Da) for the canonical nucleosides, and the major fragment ions of the reduced DOX-dR conjugates were monitored.

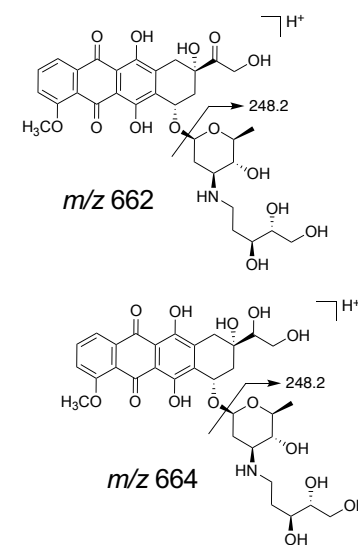
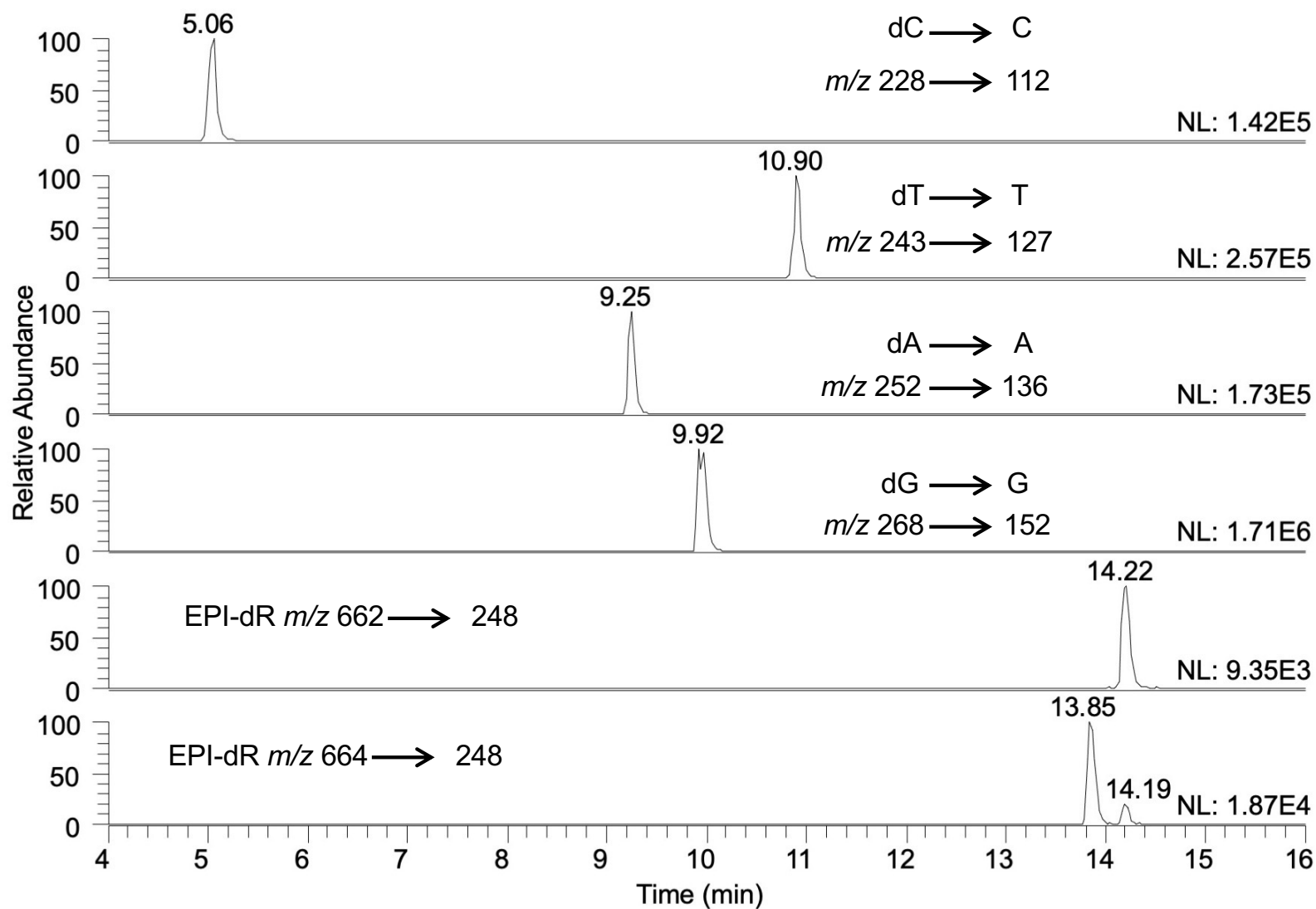


Figure S19. Extracted ion chromatograms of the enzymatic digestion of the reduced EPI-dR containing 12-mer oligonucleotide (5'-GTT GCN CGT ATG-3'). Ion trap CID was employed at the MS² scan stage to follow the loss of deoxyribose (-116 Da) for the canonical nucleosides, and the major fragment ions of the reduced EPI-dR conjugates were monitored.

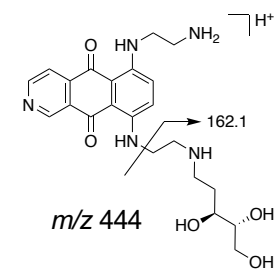
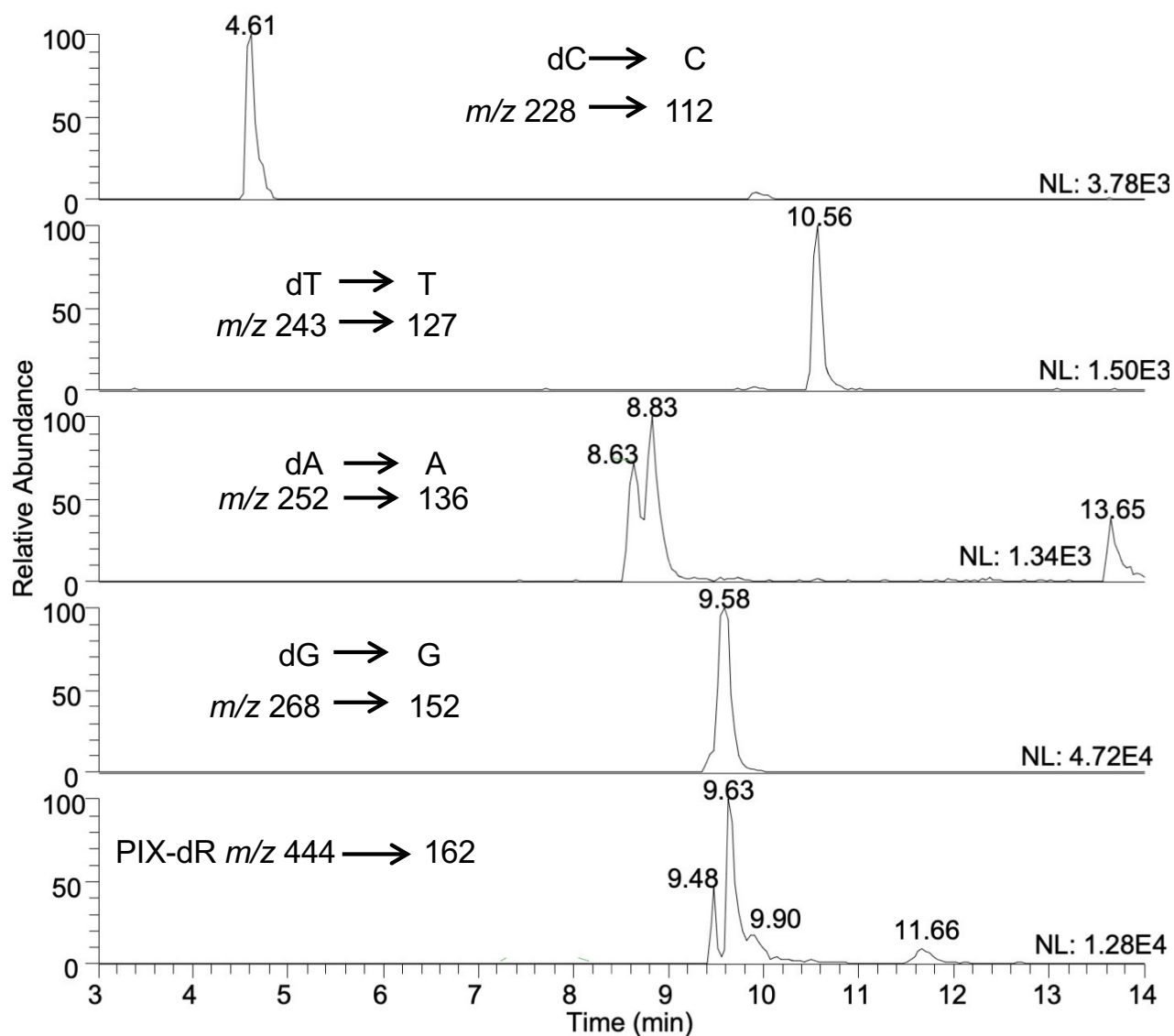


Figure S20. Extracted ion chromatograms of the enzymatic digestion of the reduced PIX-dR containing 12-mer oligonucleotide (5'-GTT GCN CGT ATG-3'). Ion trap CID was employed at the MS² scan stage to follow the loss of deoxyribose (–116 Da) for the canonical nucleosides, and the major fragment ions of the reduced PIX-dR conjugates were monitored.

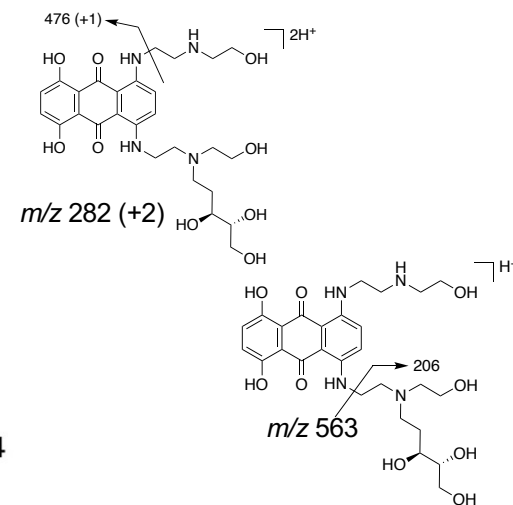
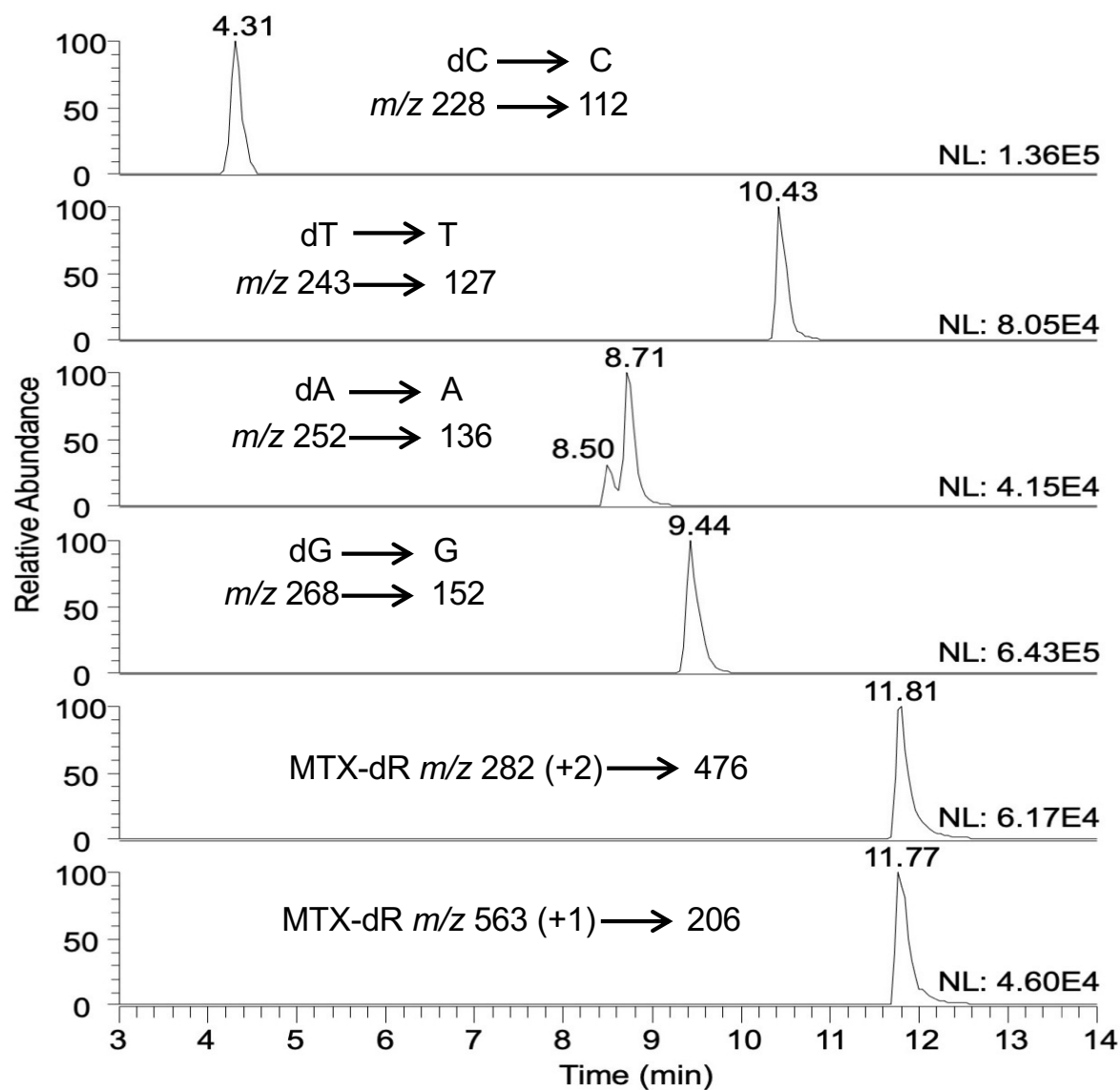


Figure S21. Extracted ion chromatograms of the enzymatic digestion of the reduced MTX-dR containing 12-mer oligonucleotide (5'-GTT GCN CGT ATG-3'). Ion trap CID was employed at the MS² scan stage to follow the loss of deoxyribose (−116 Da) for the canonical nucleosides, and the major fragment ions of the singly and doubly charged reduced MTX-dR conjugate precursor ions.

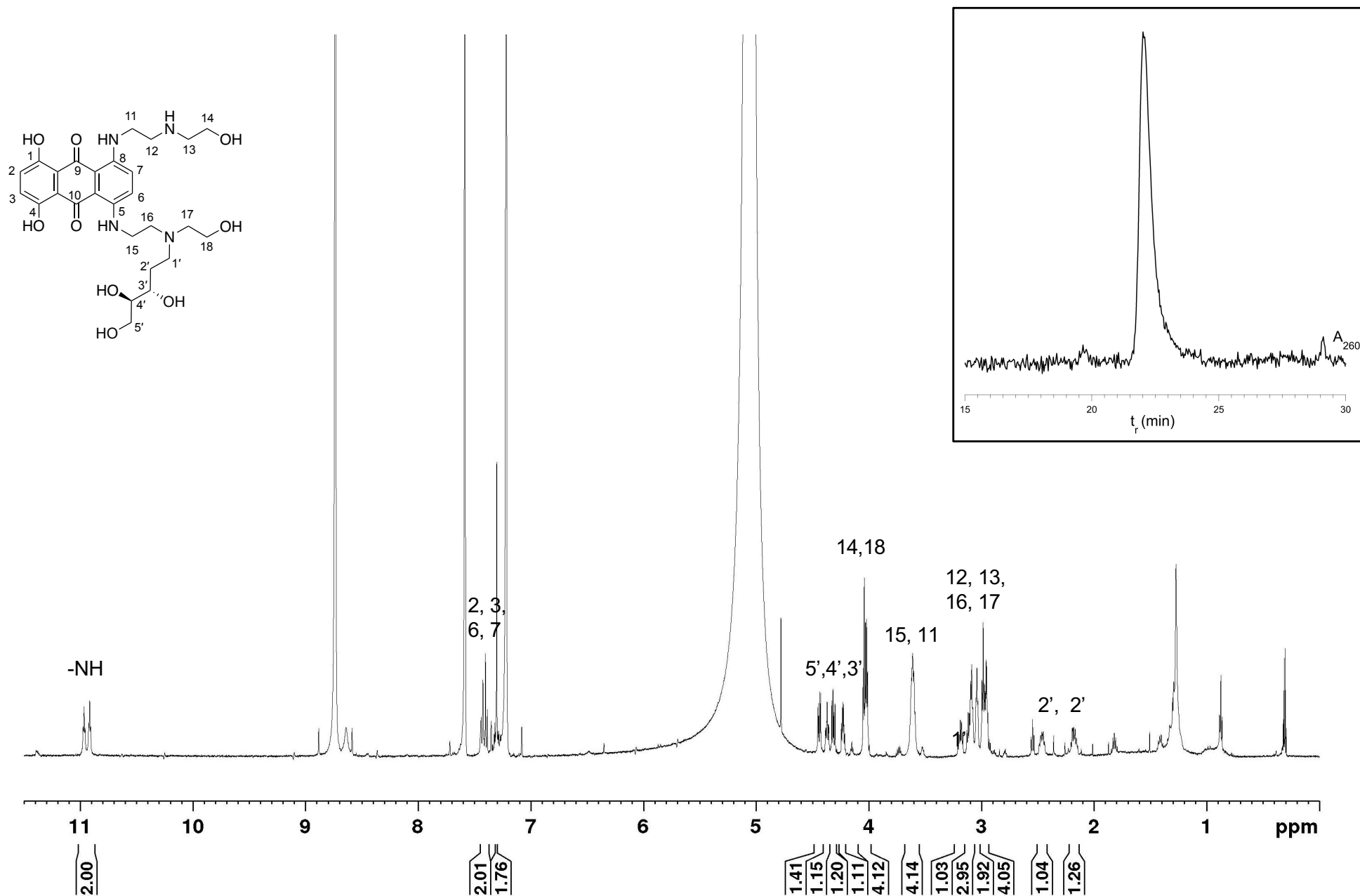


Figure S22. 600 MHz ¹H NMR spectra of reduced MTX-dR in pyridine-d₅. Inset: reversed-phase HPLC chromatogram of the purified reduced MTX-dR.

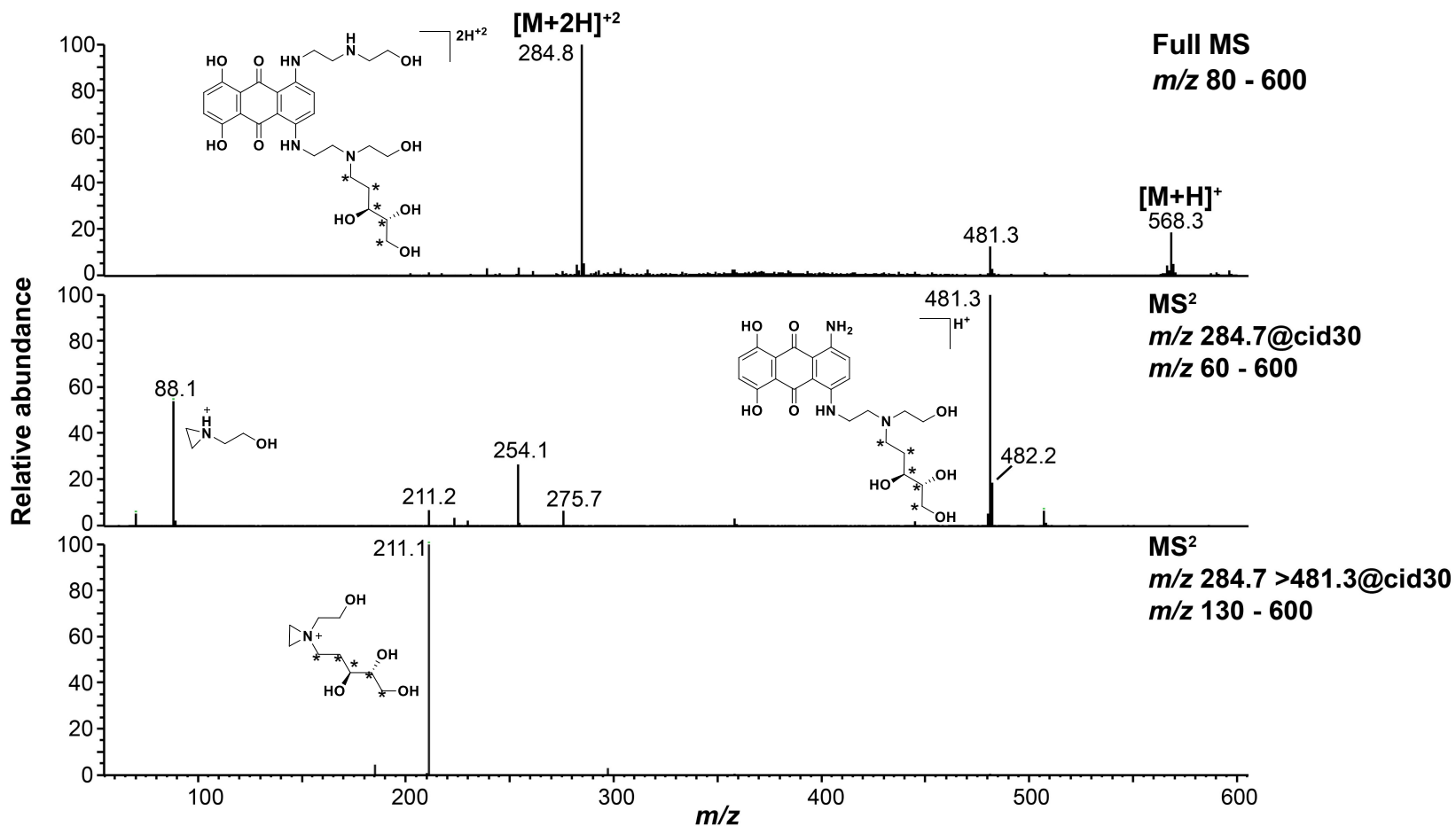


Figure S23. Full scan MS, and CID MS² and MS³ spectra of reduced MTX-[¹³C₅]-dR. The ¹³C atoms of the dR moiety are asterisked.

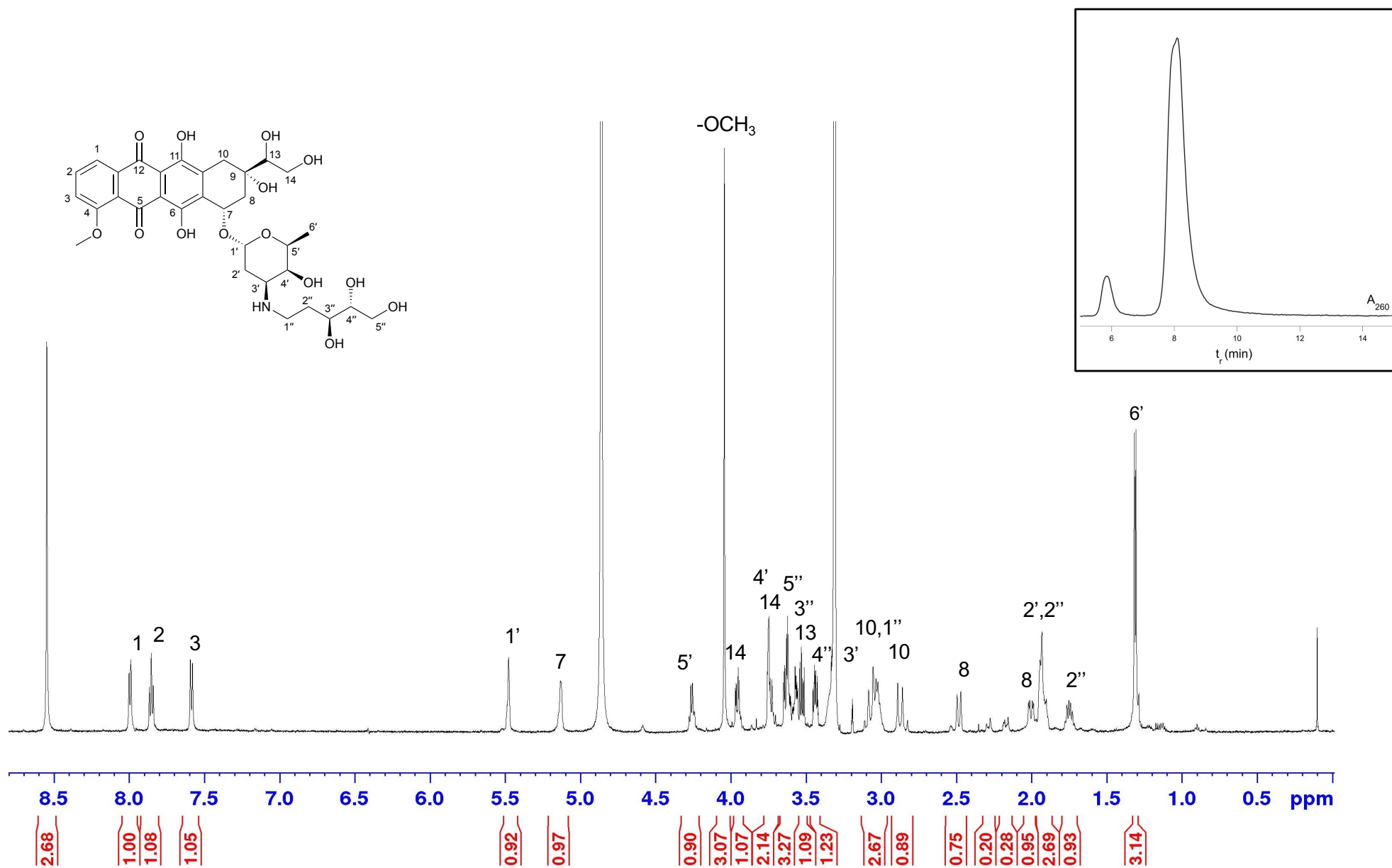


Figure S24. 600 MHz ^1H NMR spectra of reduced DOX-dR in D_3COD . Inset: reversed-phase HPLC chromatogram of the purified reduced EPI-dR. The product is a mixture of C13-alcohols.

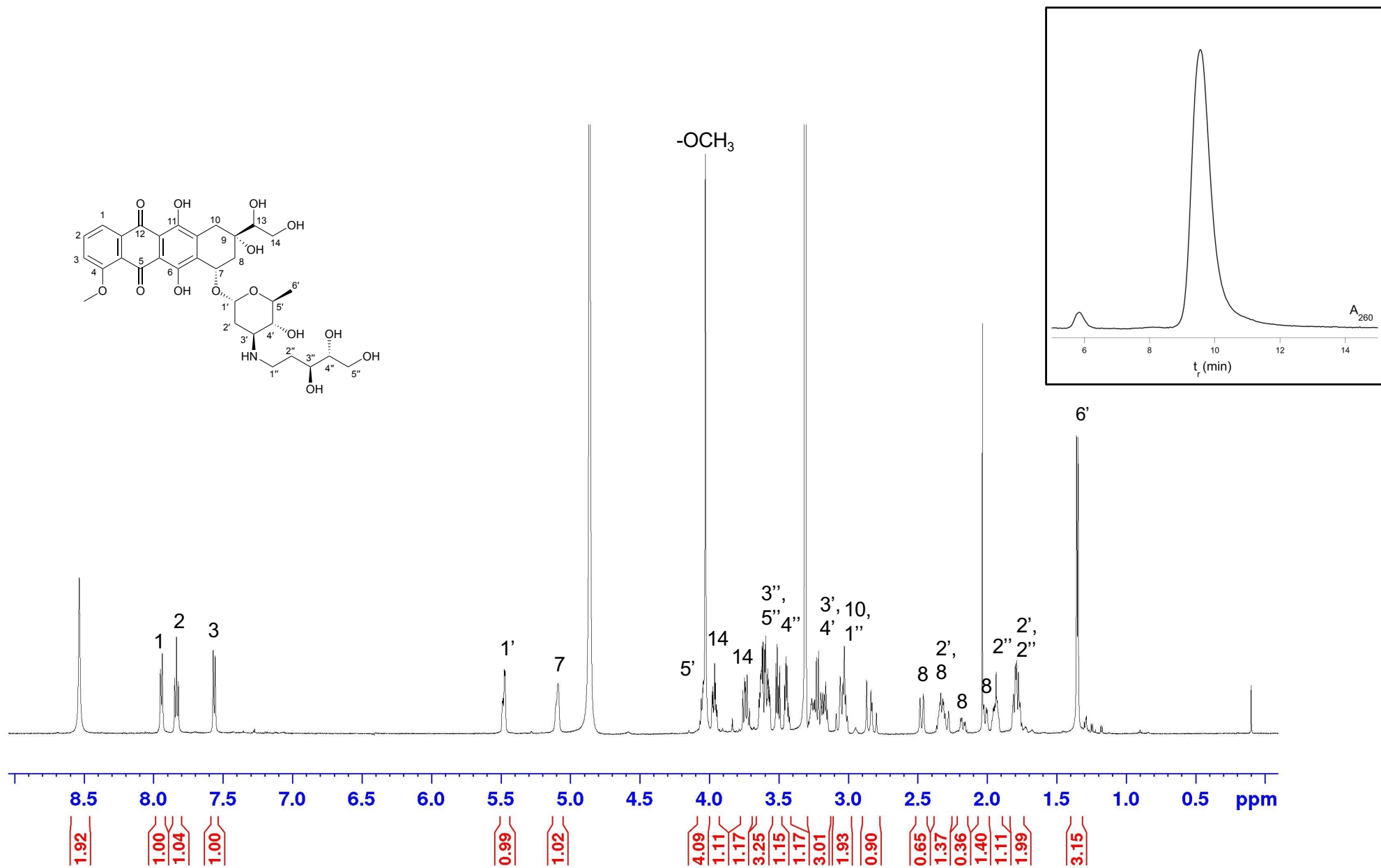


Figure S25. 600 MHz ¹H NMR spectra of the reduced EPI-dR in D₃COD. Inset: reversed-phase HPLC chromatogram of the purified reduced EPI-dR. The product is a mixture of C13-alcohols.

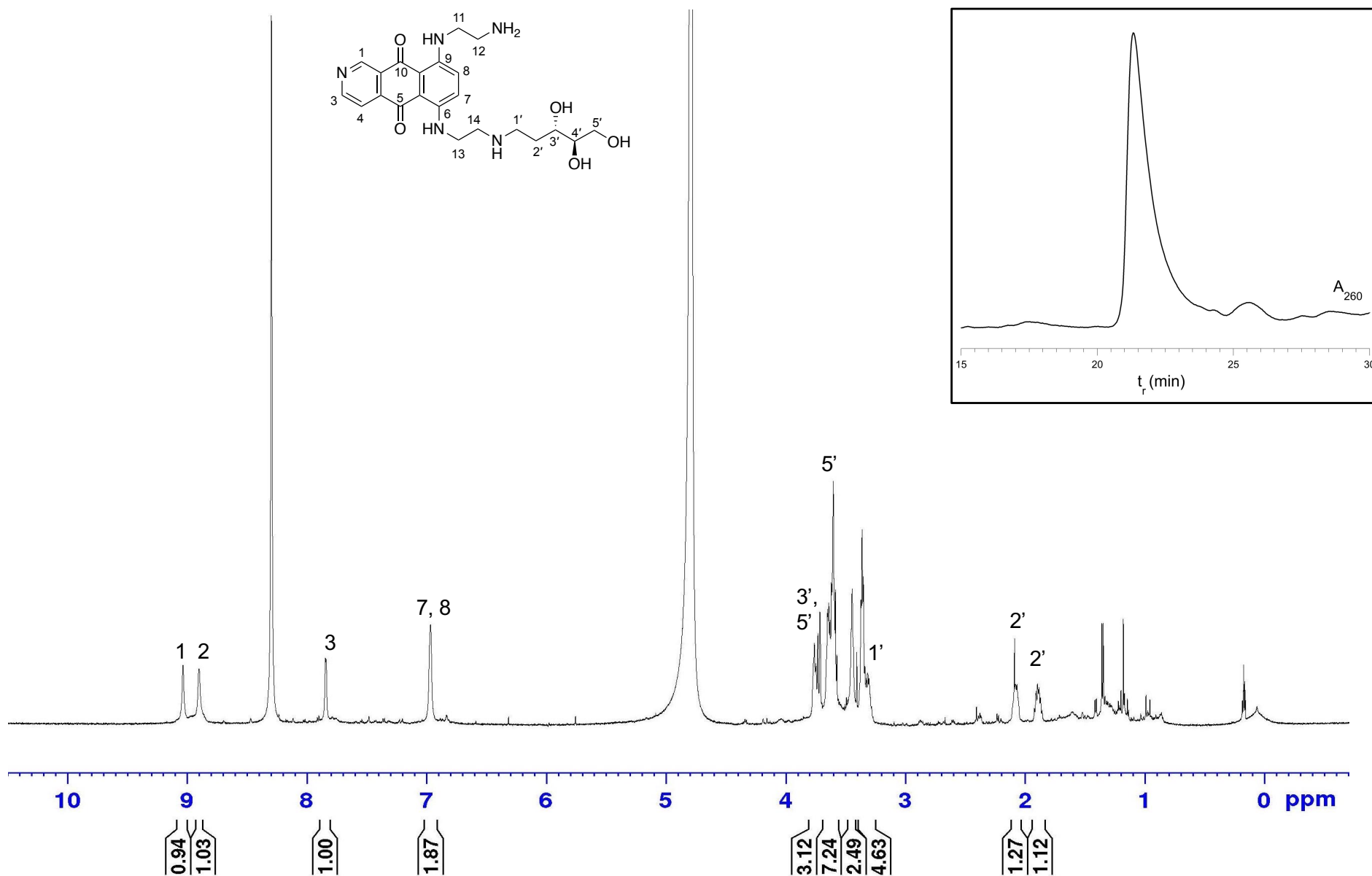


Figure S26. 600 MHz ¹H NMR spectra of the reduced PIX-dR in 0.1% DCO₂D in D₂O. Inset: reversed-phase HPLC chromatogram of the purified reduced PIX-dR. The product is a mixture of regioisomers, but only one is shown.

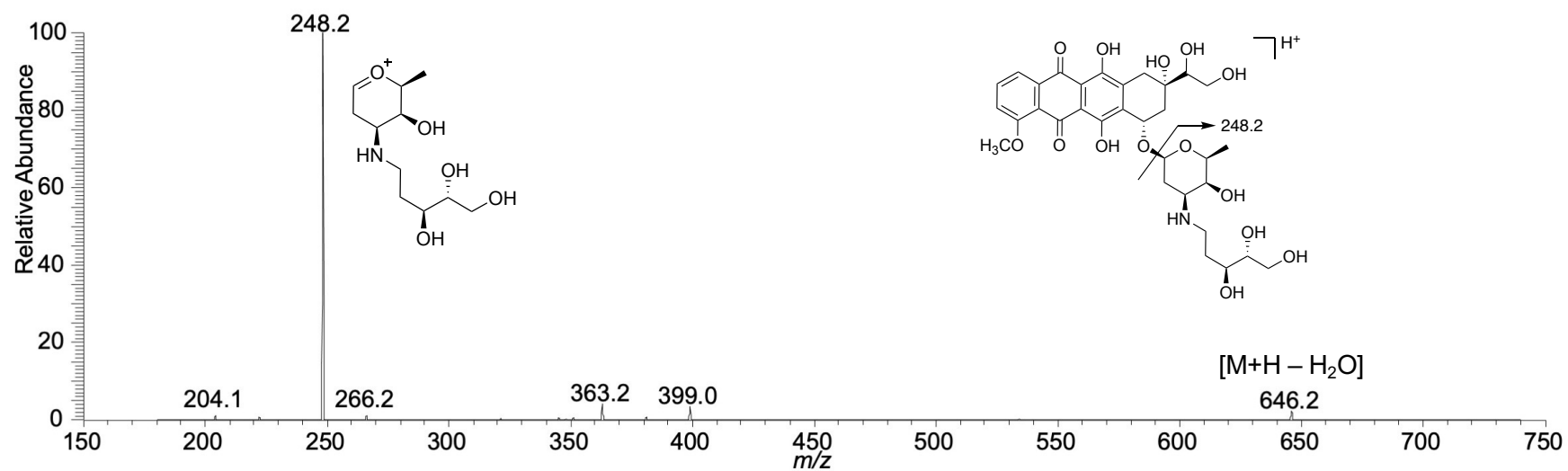
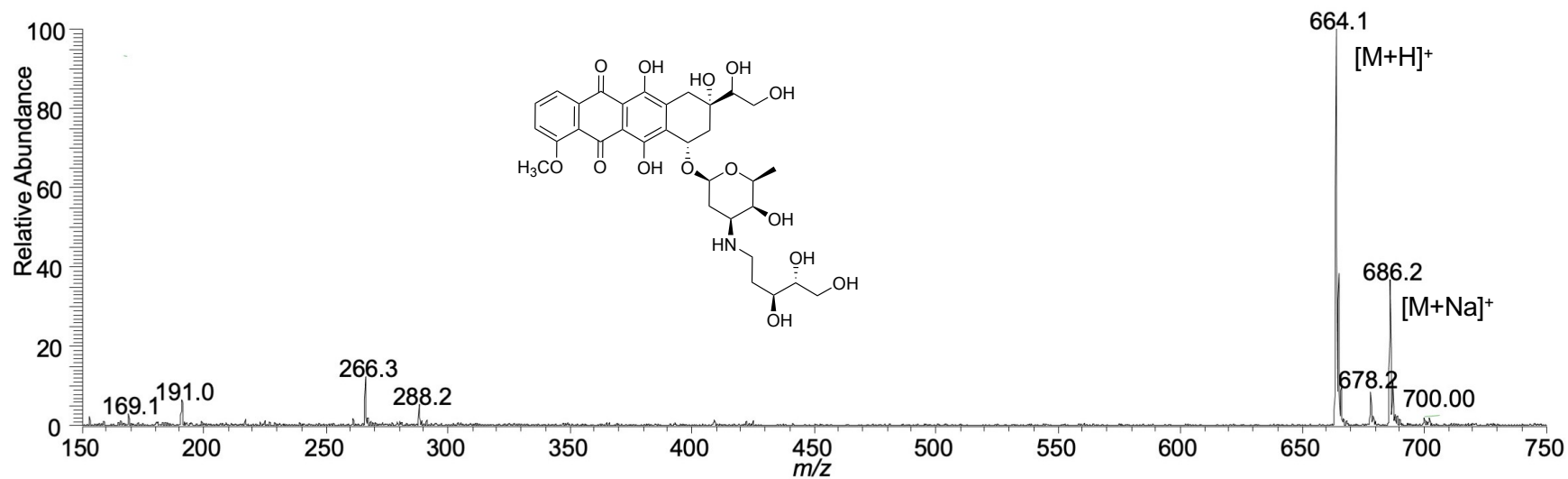


Figure S27. Full scan (top) and CID (bottom) mass spectra of reduced DOX-dR.

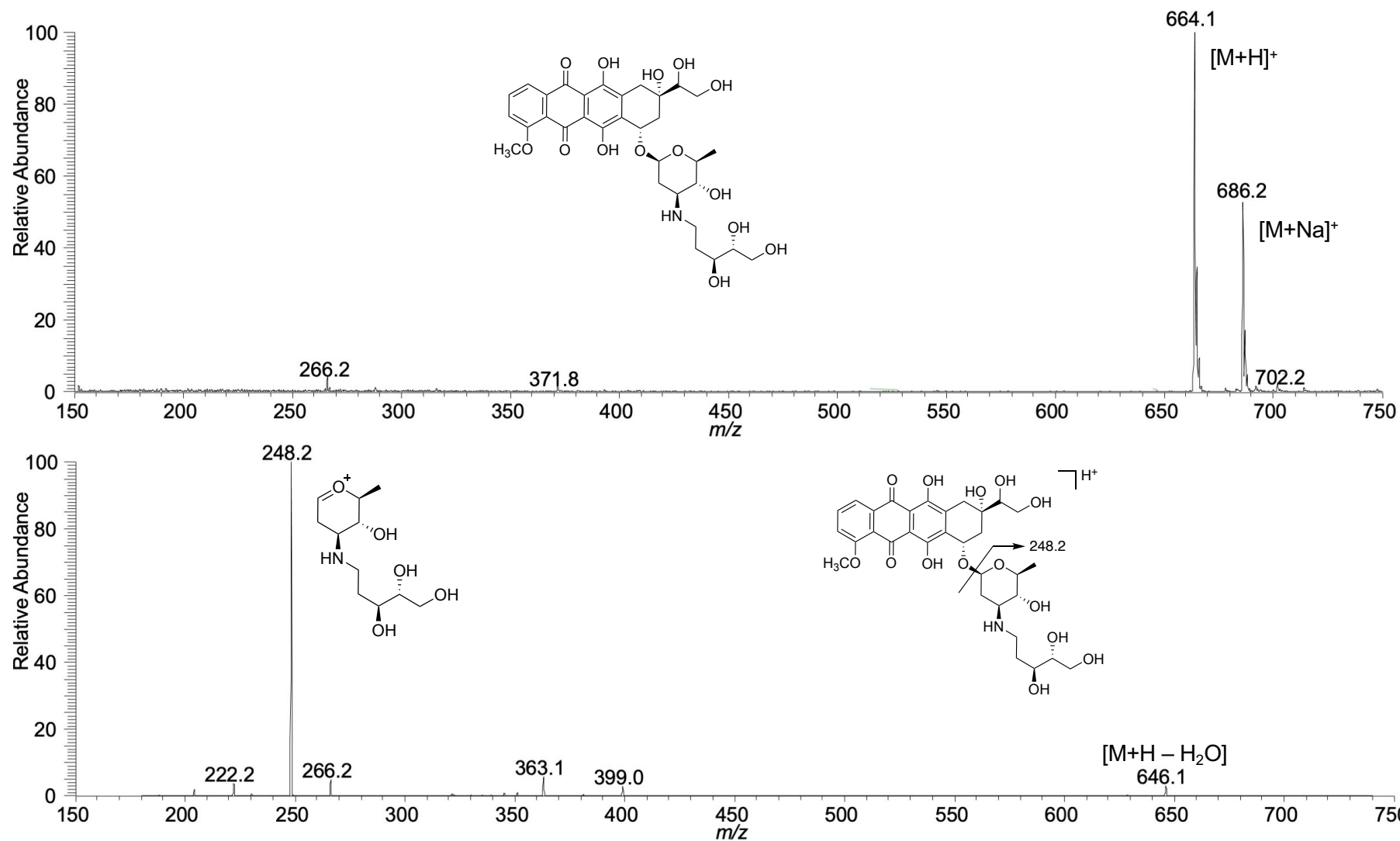


Figure S28. Full scan (top) and CID (bottom) mass spectra of the reduced EPI-dR.

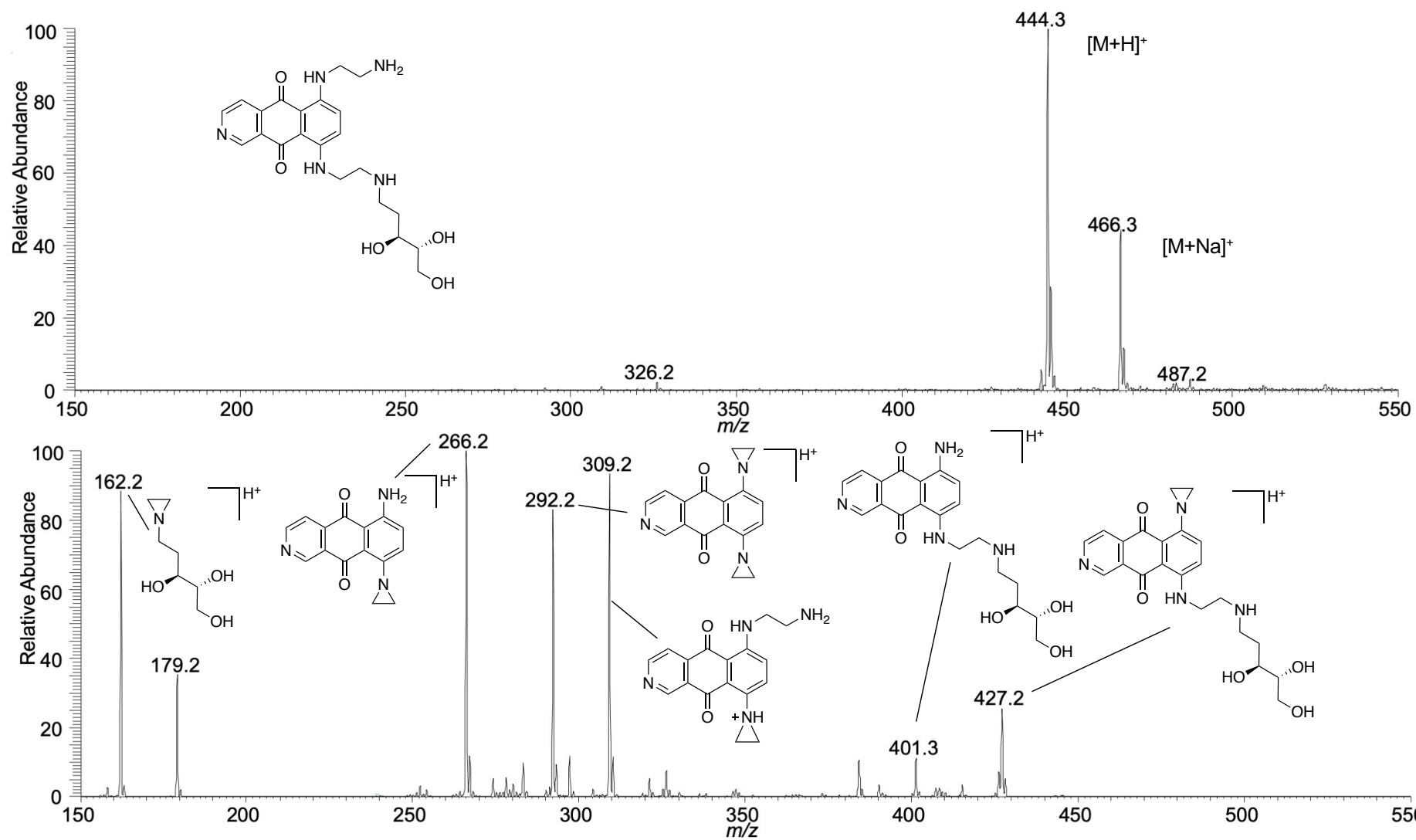


Figure S29. Full scan (top) and CID (Bottom) mass spectra (m/z 444.3 ion) of the reduced PIX-dR conjugate.

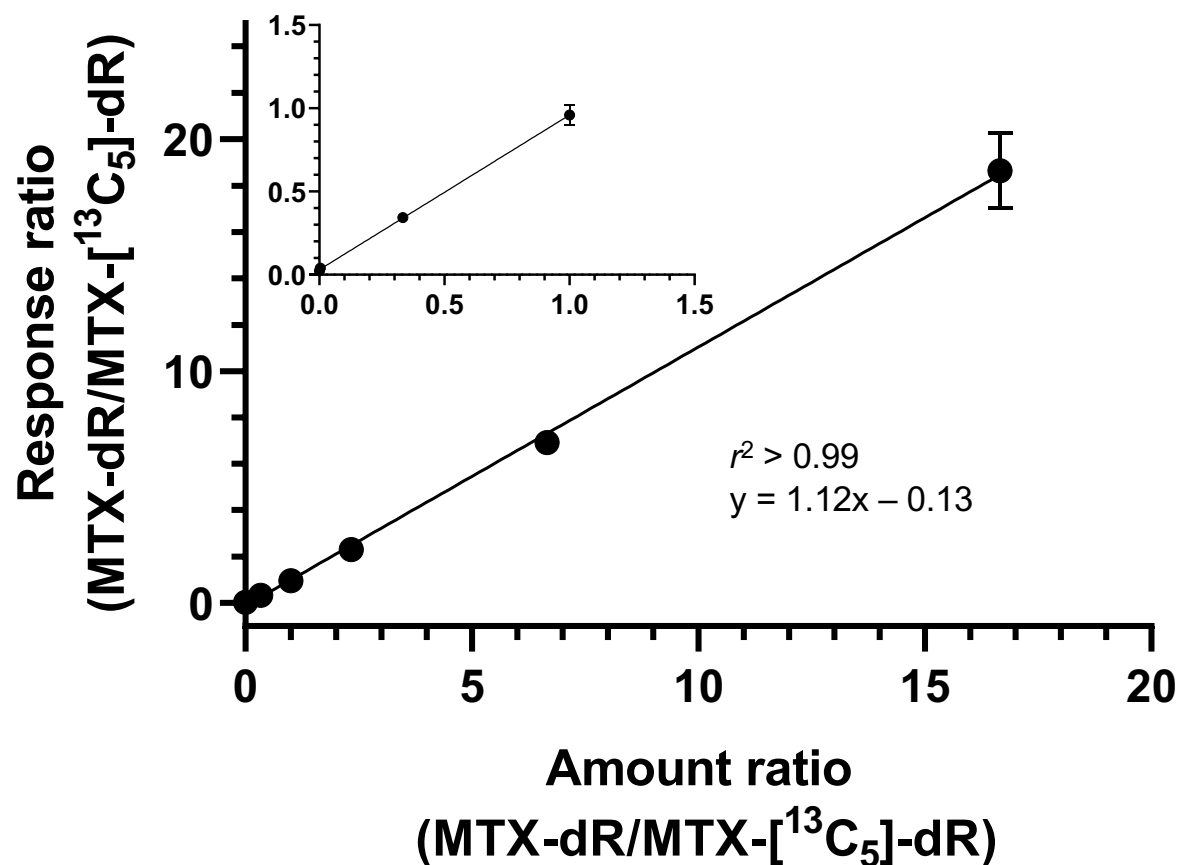


Figure S30. The calibration curve for reduced MTX-dR was constructed within a CT DNA digest matrix. CT DNA (10 μg) was spiked with 50 pg [$^{13}\text{C}_5$]-MTX-dR (2.90 adducts per 10^6 nts), and MTX-dR standard was built using seven calibrant levels ranging from 0 to 4.83 MTX-dR adducts per 10^5 nts. The CT DNA was enzymatically digested followed by MTX-dR enrichment by SPE. Each calibration level was done in quadruplicate, and the linear regression was done using ordinary least-squares with equal weighting. The calibration curve is drawn with the mean and the SD is shown when larger than the symbol; the goodness-of-fit regression value of $r^2 \geq 0.99$. The reduced MTX-dR response ratios in the cells ranged from ~ 0.3 to 5.2 (0.09 - 1.5 adducts per 10^5 nts).

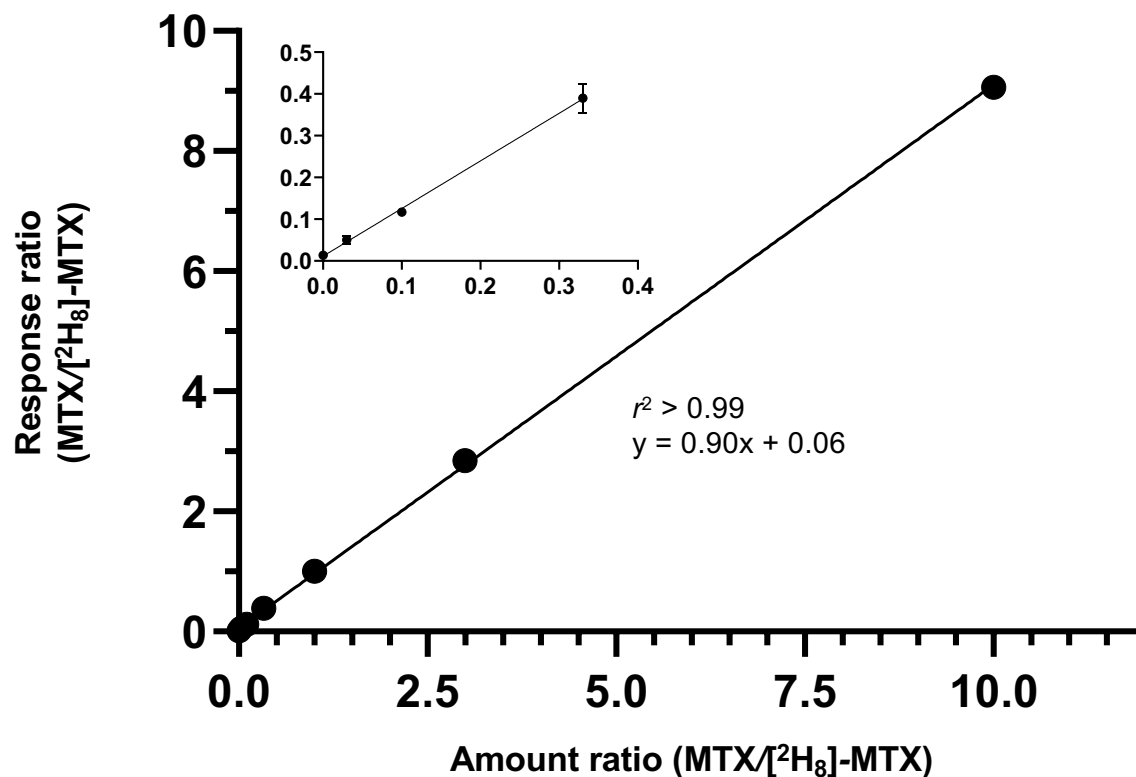


Figure S31. A calibration curve for MTX was constructed within a CT DNA digest matrix. CT DNA (10 μ g) was spiked with 0.67 ng d_8 -MTX (1.5 nmol) and unlabeled at seven calibrant levels ranging from 0, 0.01 up to 30 nmol. The CT DNA was enzymatically digested and MTX was enriched by SPE. Each calibration level was done in triplicate, and the linear regression was done using ordinary least-squares with equal weightings. The calibration curve is drawn with the mean (the SD is smaller than the symbols for most data points); the goodness-of-fit regression value of $r^2 \geq 0.99$. The uptake of MTX ($\sim 20 - 25\%$ of the dose given) resulted in response ratios ranging from ~ 0.15 to 10.0. We assumed that 10 μ g is the approximate amount of DNA present in one million MDA-MB-231 cells.

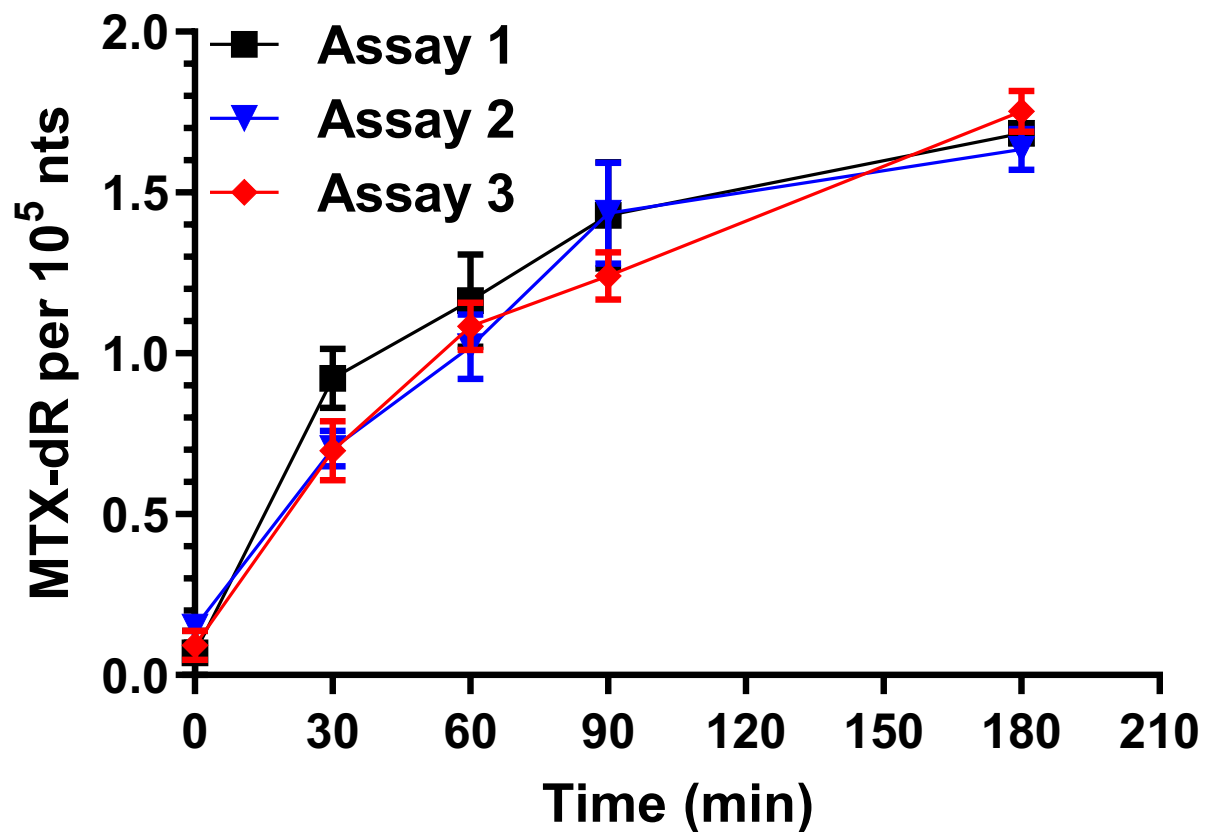


Figure S32. Kinetics of MTX-dR Schiff base formation in CT DNA reduced with NaB(CN)H₃. CT DNA in 100 mM HEPES pH 7.4, 10 mM NaCl was treated with MTX for 2.5 h, followed by reduction with NaB(CN)H₃ (100 mM). Time 0 is the addition of the reducing agent, and the time of reduction was up 3 h. Adduct levels are reported as the mean \pm SD ($n = 3$ replicates and three independent assays). AP site levels in CT DNA range between 1.5 – 2.0 AP sites per 10⁵ nts.

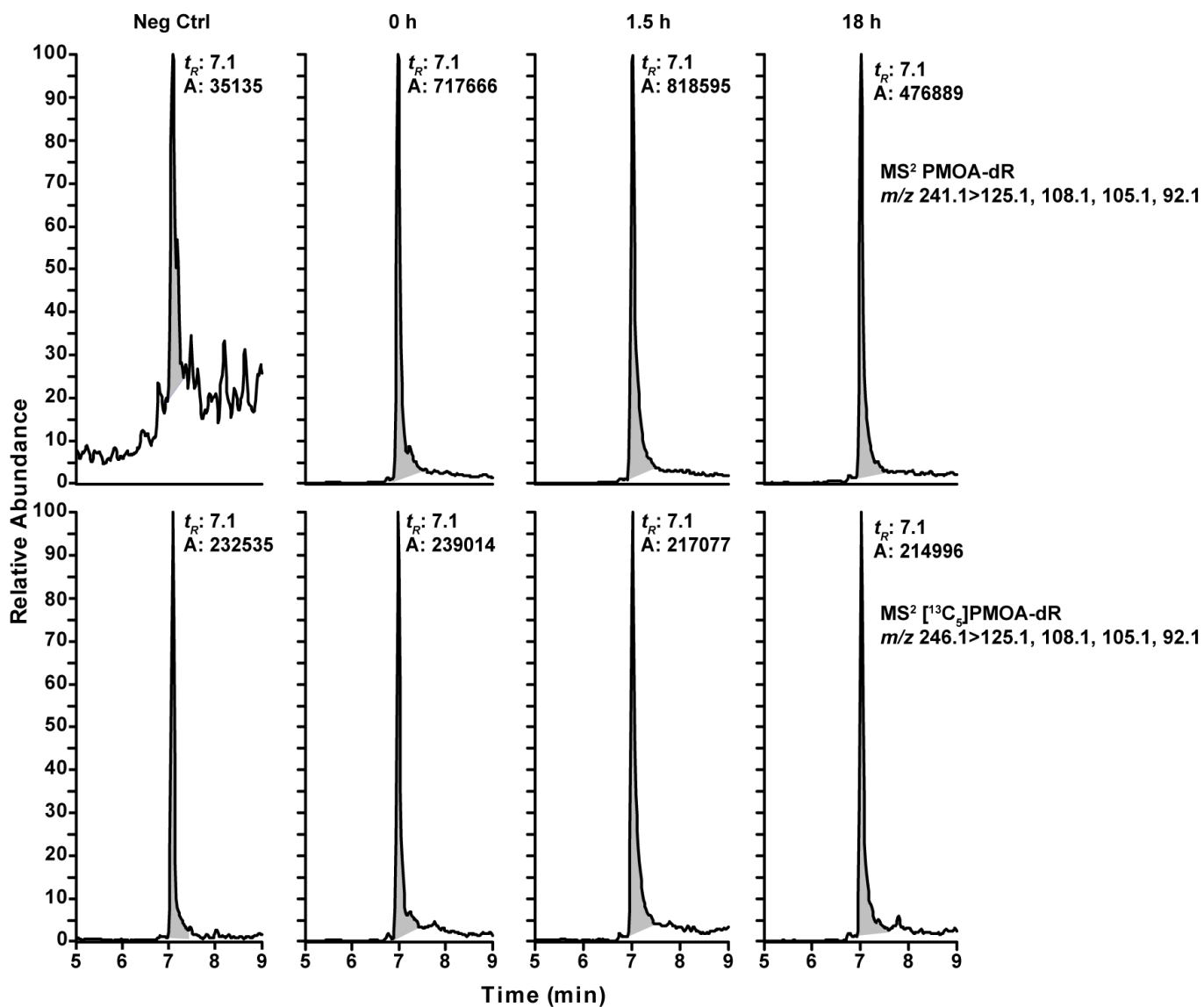


Figure S33. AP Site formation in MDA-MB-231 breast cancer cell line over time after co-treatment with 1 mM NNM and 0.6 μ M MTX followed by monitoring AP sites levels in the isolated nuclei after reduction with NaB(CN)₃ for up to 18 h by LC/MS². The EICs of PMOA-dR and [¹³C₆]PMOA-dR are shown.

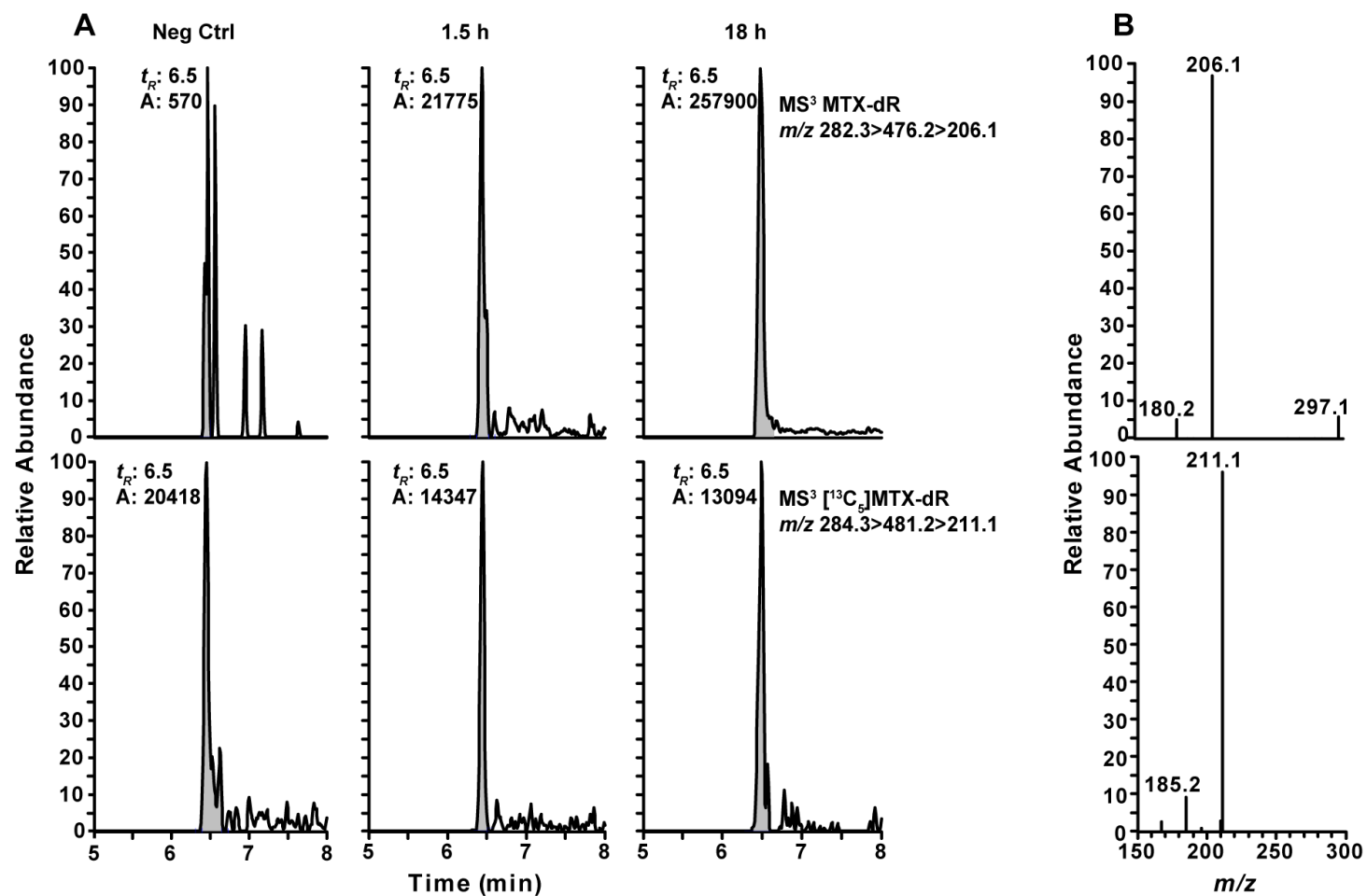


Figure S34. Reduced MTX-dR levels formed over time in NNM and MTX treated MDA-MB-231 cells isolated nuclei. Following 24 h of co-treatment with 1 mM NNM and 0.6 μ M MTX, nuclei were isolated and treated with NaB(CN)H₃ for up to 18 h. The EICs and product ion spectra of reduced MTX-dR and its internal standard at the MS³ scan stage are shown. (A) Negative control cells reduced with NaB(CN)H₃ for 18 hr, and NNM/MTX-treated cells reduced with NaB(CN)H₃ for 1.5 h and 18 h.

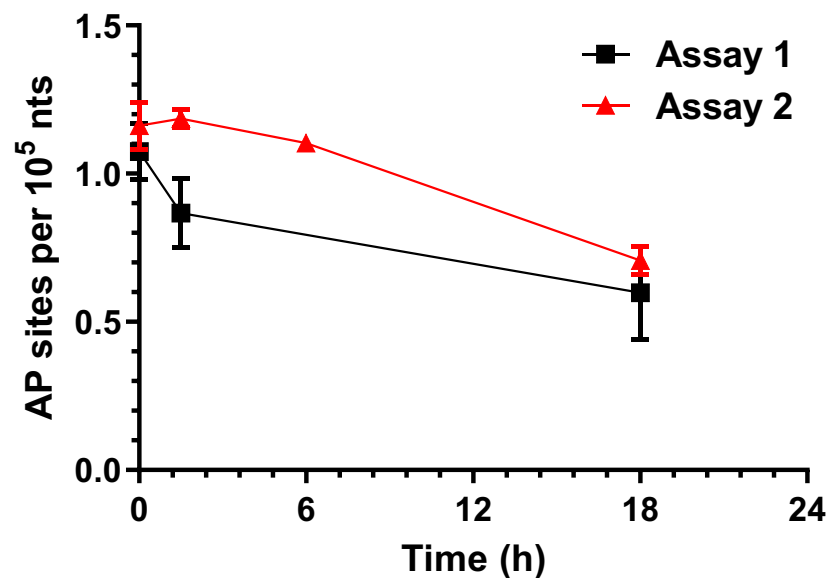
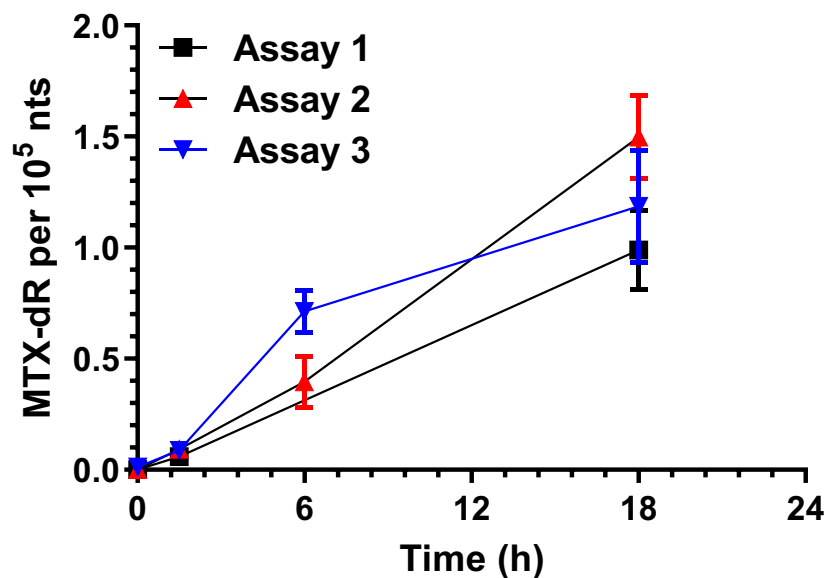


Figure S35. MDA-MB-231 cells co-treated with 1 mM NNM and 0.6 μ M MTX for 18 h. Reduced MTX-dR levels formed over time in the isolated nuclei treated $\text{NaB}(\text{CN})\text{H}_3$. AP site levels and stability in the nuclei of untreated and NNM/MTX treated cells were measured at the same time points as for reduced MTX-dR. Adduct levels are reported as the mean \pm SEM ($n = 4$ independent replicates).

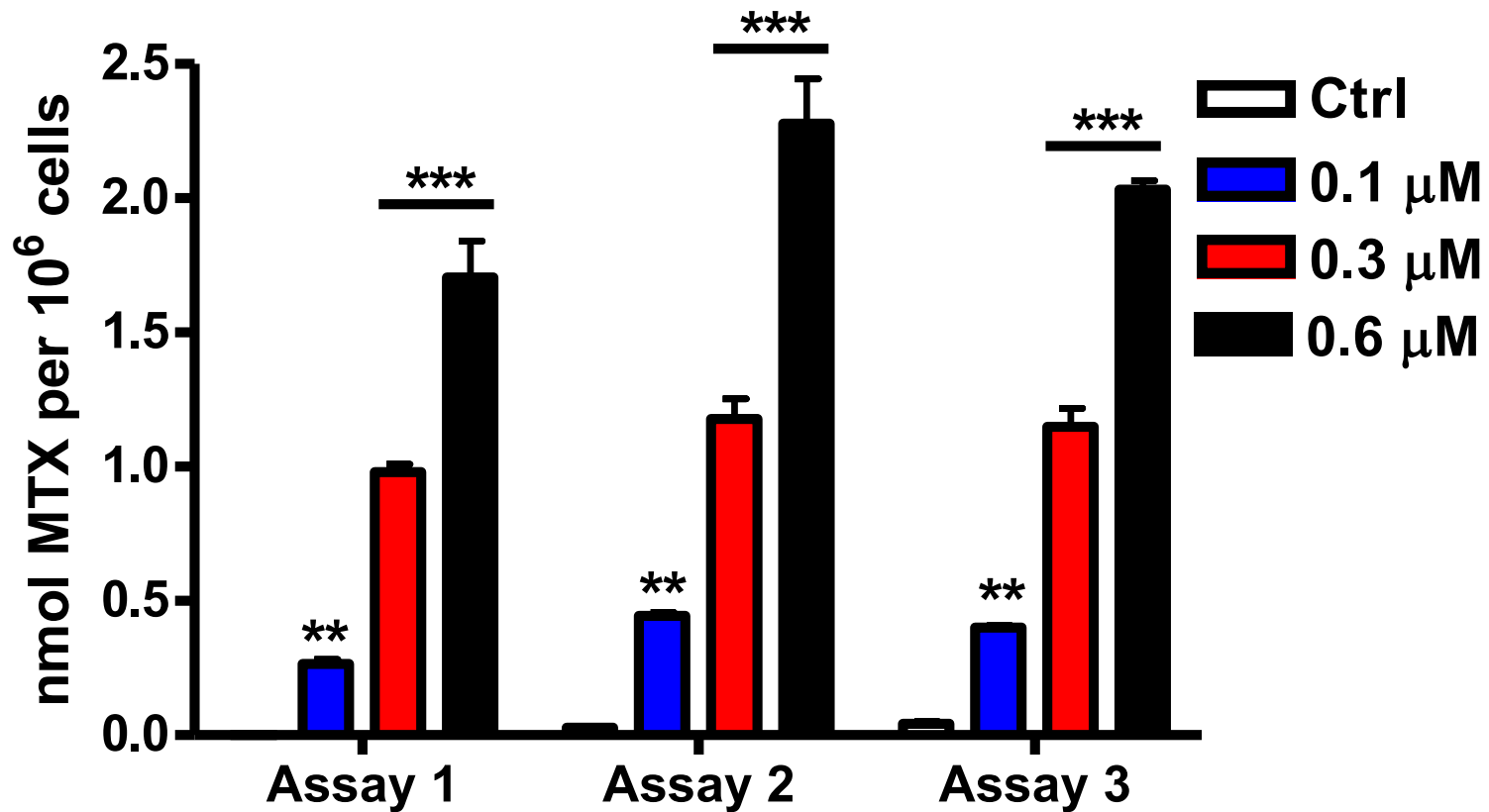


Figure S36. MTX uptake in nuclei isolated from MDA-MB-231 cells treated with various concentrations of MTX for 24 h. The amount (nmol) of MTX is expressed per 10⁶ cells. (**P* < 0.05; ***P* < 0.01, ****P* < 0.005). Three independent assays were performed.

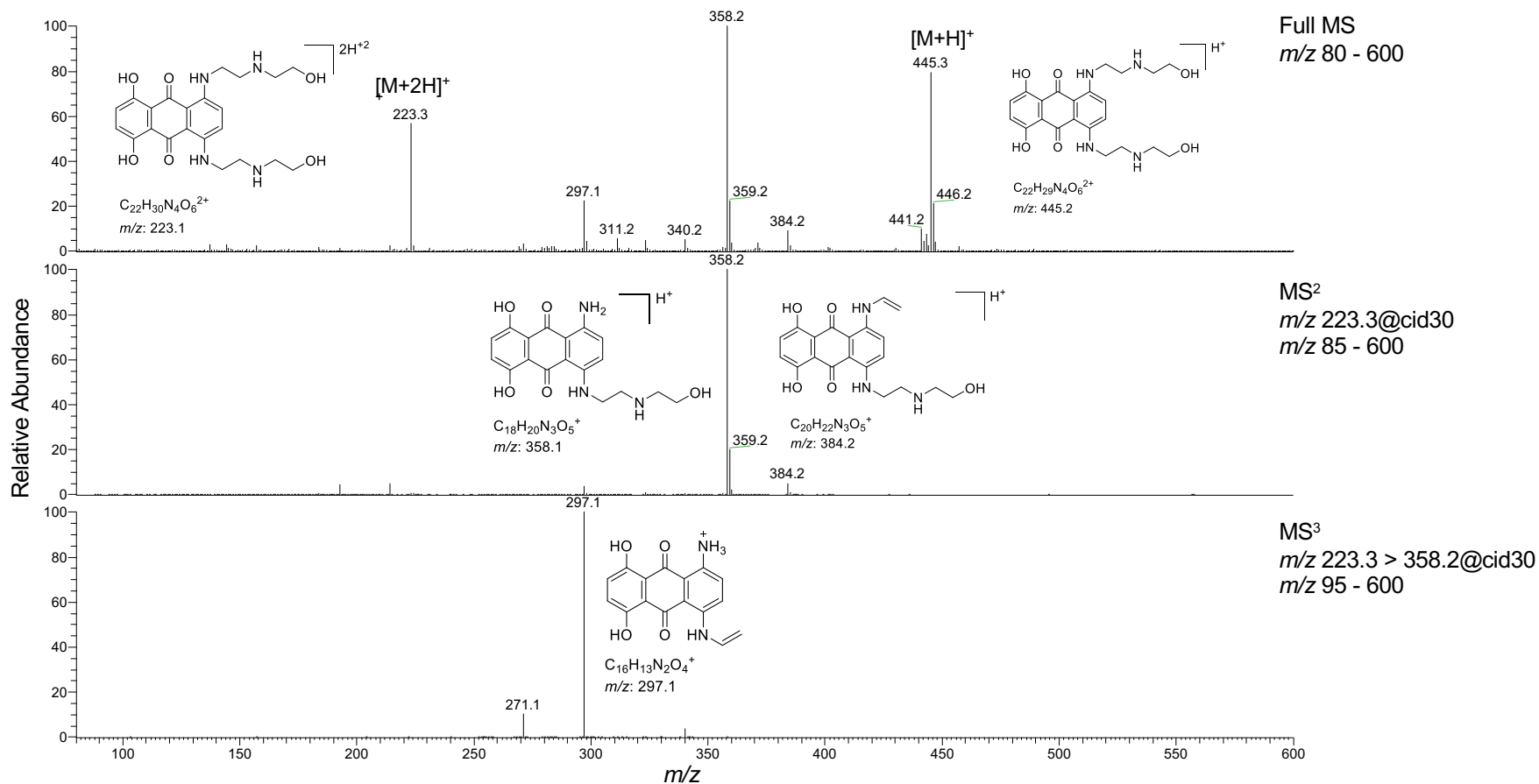


Figure S37. (A) Full-scan spectrum of the MTX showing the singly protonated $[M+H]^+$ at m/z 445.3, and the doubly protonated $[M+2H]^{2+}$ ion at m/z 223.3. (B) The CID MS² scan stage mass spectrum of m/z 223.3 and (C) MS³ spectrum of the m/z 358.2 product ion are reported.

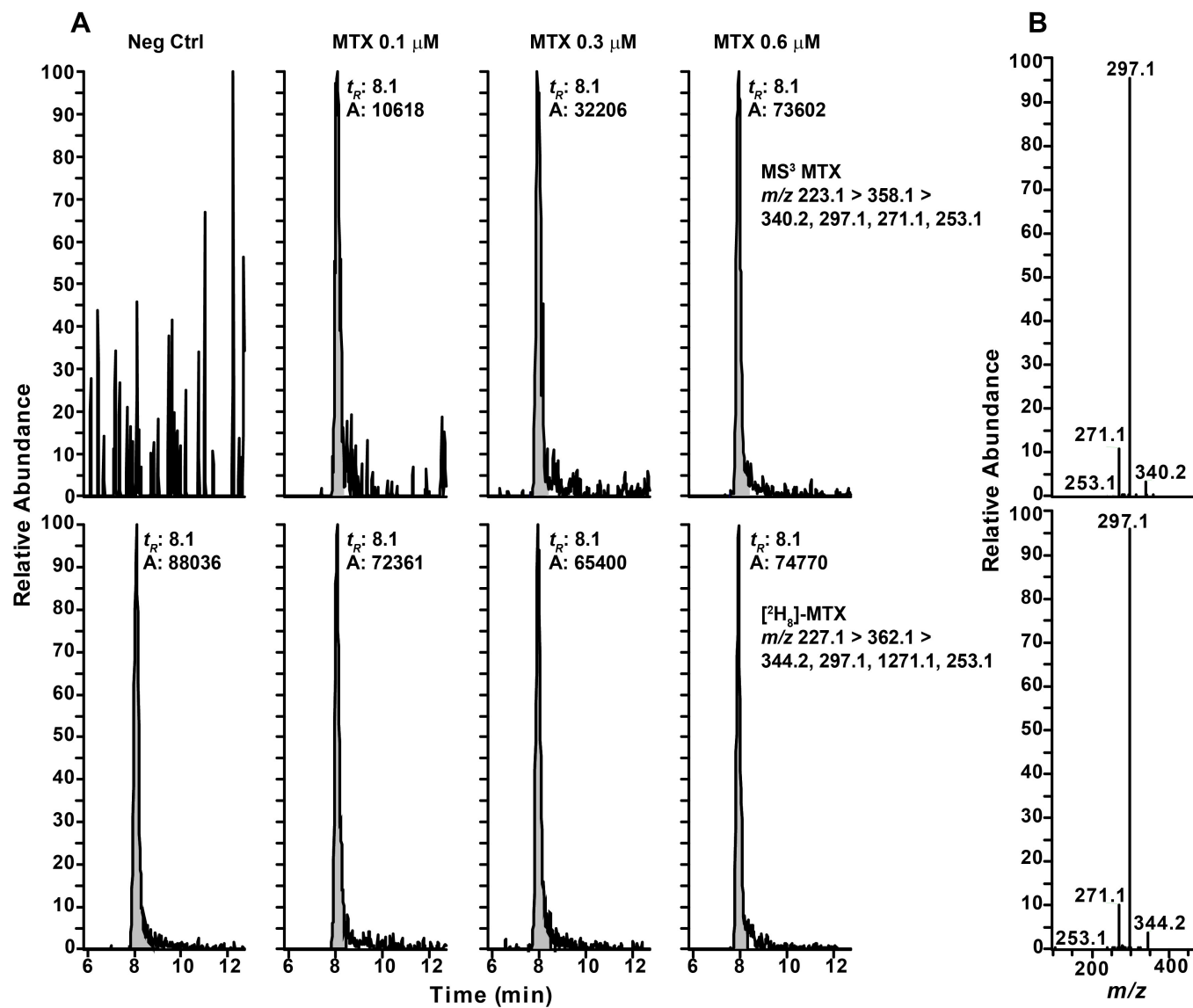


Figure S38. MTX uptake in MDA-MB-231 breast cell line after 24 h of MTX treatment (0.1, 0.3, and 0.6 μM). (A) LC/MS³ EICs of MTX levels uptaken in the nuclei. (B) CID MS³ spectra of MTX and [²H₈]MTX.

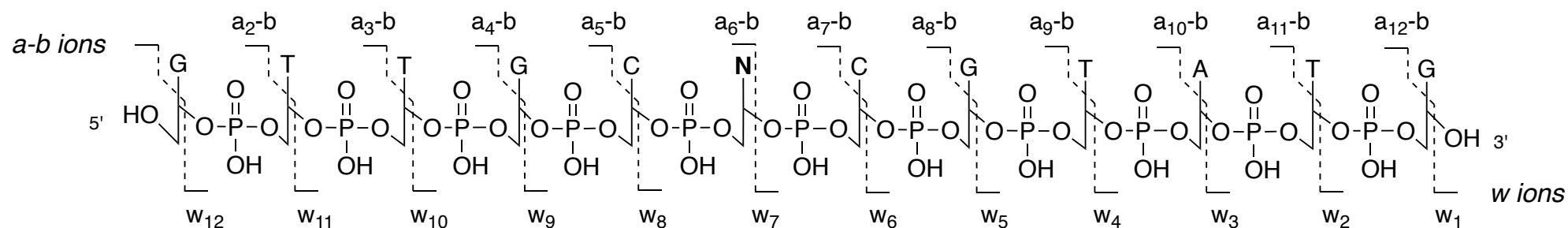


Figure S39. MS fragment ion nomenclature for oligonucleotides (see: McLuckey, S. A., Van Berker, G. J., and Glish, G. L. (1992) Tandem mass spectrometry of small, multiply charged oligonucleotides. *J. Am. Soc. Mass. Spectrom.*, 60–70). All oligonucleotide masses were calculated using the Mongo Oligo Mass Calculator, v. 2.06 (<http://rna.rega.kuleuven.be/masspec/mongo.htm>).